

General Disclaimer

One or more of the Following Statements may affect this Document

- This document has been reproduced from the best copy furnished by the organizational source. It is being released in the interest of making available as much information as possible.
- This document may contain data, which exceeds the sheet parameters. It was furnished in this condition by the organizational source and is the best copy available.
- This document may contain tone-on-tone or color graphs, charts and/or pictures, which have been reproduced in black and white.
- This document is paginated as submitted by the original source.
- Portions of this document are not fully legible due to the historical nature of some of the material. However, it is the best reproduction available from the original submission.



20660-FR1

Final Report

THE DESIGN AND BUILD OF A GAS BEARING GYROSCOPE
POSSESSING HIGH-G AND STERILIZATION CAPABILITY
AND UTILIZING A LOW-POWER GAS BEARING SPIN-
MOTOR AND HIGH-FREQUENCY PUMP

Jet Propulsion Laboratory
California Institute of Technology
Pasadena, California

JPL Contract 951559

31 October 1968

N 69-16670

(ACCESSION NUMBER)	(THRU)
54	1
(PAGES)	(CODE)
OR 73647	14
(NASA CR OR TMX OR AD NUMBER)	(CATEGORY)

FACILITY FORM 602

HONEYWELL Aerospace Division



20660-FR1

31 October 1968

FINAL REPORT

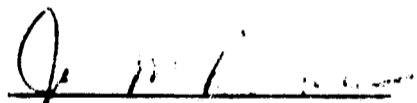
THE DESIGN AND BUILD OF A GAS BEARING GYROSCOPE POSSESSING
HIGH-G AND STERILIZATION CAPABILITY AND UTILIZING A LOW-
POWER GAS BEARING SPINMOTOR AND HIGH-FREQUENCY PUMP

Jet Propulsion Laboratory
California Institute of Technology
Pasadena, California

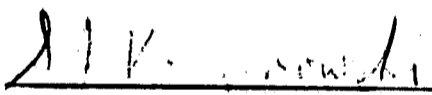
JPL Contract 951559


This work was performed for the Jet Propulsion Laboratory
California Institute of Technology, sponsored by the National
Aeronautics and Space Agency under Contract NAS7-100.

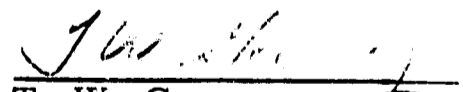
Prepared by:


J. M. Bremer
Senior Development
Engineer

Approved by:


S. J. Korzenowski
Project Engineer


R. G. Baldwin
Section Head


T. W. Garvey
Program Administrator

Honeywell Inc.
Aerospace Division
Minneapolis, Minnesota

NOTICE

This report was prepared as an account of Government-sponsored work. Neither the United States, nor the National Aeronautics and Space Administration (NASA), nor any person acting on behalf of NASA:

- a. Makes warranty or representation, expressed or implied, with respect to the accuracy, completeness, or usefulness of the information contained in this report, or that the use of any information, apparatus, method, or process disclosed in this report may not infringe privately-owned rights; or
- b. Assumes any liabilities with respect to the use of, or for damages resulting from the use of any information, apparatus, method, or process disclosed in this report.

As used above, "person acting on behalf of NASA" includes any employee or contractor of NASA, or employee of such contractor, to the extent that such employees or contractor of NASA, or employee of such contractor prepares, disseminates, or provides access to, any information pursuant to his employment with such contractor.

Request for copies of this report should be referred to:

National Aeronautics and Space Administration
Office of Scientific and Technical Information
Washington 25, D. C.

Attention: AFSS-A

TABLE OF CONTENTS

		Page
SECTION I	SUMMARY	1
	Historical Perspective	10
	Organization of Report	10
SECTION II	HIGH-G CAPABILITY -- LOW-POWER MOTOR DEVELOPMENT	12
	Gas Bearing Spinmotor (GBSM) Design -- First Iteration	12
	Initial Gas Bearing Spinmotor Tests	14
	Final GBSM Design	19
	Gyro Test Results	19
SECTION III	HIGH-FREQUENCY PUMP	21
	Cartridge Pump Design	21
	Suspension Fluid Search	26
	Suspension Damping	28
	Gyro Redesign	28
	Test Results in the Gyro	31
SECTION IV	STERILIZATION CAPABILITY	32
	Spinmotor Materials	
	Lockup	33
	Assymetrical Journal Pattern	33
	Particulate Contamination	34
	Stator Canning	35
	New Header Design	38
	Sterilization Test Results	38
SECTION V	CONCLUSIONS	48

LIST OF ILLUSTRATIONS

Figure		Page
1	Schematic Diagram	7
2	Installation Drawing	8
3	GG159E Anisoelastic Coefficient	9
4	Low-Power Spinmotor Configuration	13
5	GG159 Thrust Bearing Frequency Response	15
6	GG334 Thrust Bearing Frequency Response	16
7	GG159E Bearing Displacement versus Shock Magnitude	17
8	GG159E Bearing Displacement versus Shock Magnitude	18
9	High-Frequency Pump Layout	22
10	Piezo Pumping Plate Assembly	24
11	Piezo Pump Pressure and Flow versus Frequency	25
12	Gimbal Suspension Damping over the 50°F to 130°F Range	29
13	Piezoelectric Pump Life Test	30
14	GG159E Gimbal Gas Sampling Fixture	36
15	GG159E Contamination	37
16	Infrared Spectrum of GG159E Contamination	39
17	Encased and Standard Motor Stator	40
18	Bellows Travel versus Gyro Temperature	41
19	Balance Torque History	43
20	Step Response	44

LIST OF TABLES

Table		Page
I	Sterilization Testing	2
II	High-g Test Results	2
III	Mechanical and Performance Characteristics	3
IV	Performance Parameters	4
V	Excitations Required	5
VI	Current Resistances and Inductances	6
VII	Area and Drag Parameters	14
VIII	GBSM Magnetics Test Results	20
IX	Results of Three High-Frequency Pump Mounting Schemes	23
X	Materials in GBSM	32
XI	Moisture Lockup Sensitivity of Optimized Assymetrical Journal Design	34
XII	General Test Results	45
XIII	Sterilization Test Results	47

SECTION I SUMMARY

This final report is submitted in fulfillment of JPL Contract 951559. The program objective was to design and to fabricate a gyroscope which would incorporate the following major design goals:

- Sterilization capability
- High-g capability
- Low-power spinmotor
- High-frequency fluid pump

The program was completed with the shipment of one Model GG159E1 gyro, S/N B1, to JPL on 9 September 1968. This unit essentially met most of the design goals for performance over sterilization as seen by a comparison of the goals with the actual results in Table I. The high-g capability of the gyro was verified by the test results presented in Table II. The spinmotor required 3.5 watts running power, which was well below the 4.0-watt contract requirement. Moreover, the ability to build a spinmotor requiring less than 3.0 watts was concurrently demonstrated. The fluid pump operated at 490 Hz, against the contract requirement of 400 Hz.

The as-shipped unit satisfied the four major design goals stated above. The unit easily demonstrated the ability to withstand the environmental exposures and proved itself to be a good, accurate inertial sensor. Further specific details pertaining to the unit are included in this report as follows:

- Table III - Mechanical and Dynamic Characteristics
- Table IV - Performance Parameters
- Table V - Excitation Requirements
- Table VI - Circuit Resistances and Inductances
- Figure 1 - Schematic Diagram
- Figure 2 - Installation Drawing
- Figure 3 - Anisoelastic Coefficient versus Frequency

Two difficulties with the hardware (not directly related to performance) did occur during sterilization. These were (1) an open SMRD winding and (2) decreased balance pan sensitivity.

Table I. Sterilization Testing

Parameter	Design Goal (Each Cycle)	Test Result
Change in TSF	± 4.0 deg/hr/ma	0.065 deg/hr/ma Total
Change in MU_{SRA}	± 0.14 deg/hr/g	0.105 deg/hr/g (AVG); 0.198 deg/hr/g max
Change in MU_{IA}	± 0.14 deg/hr/g	0.100 deg/hr/g (AVG); 0.202 deg/hr/g max
Change in RT (total)	± 0.07 deg/hr	0.075 deg/hr (AVG); 0.095 deg/hr max*
Change in Elastic Restraints	± 0.015 deg/hr/mr	0.006 deg/hr/mr max spread

*Excluding first point as not representative. Including this point, the values would be 0.215 (AVG); 0.529 max.

Table II. High-g Test Results

Environment	ΔRT (deg/hr)	ΔFT (deg/hr)	ΔMU_{IA} (deg/hr/g)	ΔMU_{SRA} (deg/hr/g)
Shock (200 g, 1.5 ms, 5 each along major axes)	-0.10	+0.01	+0.63	-0.24
Shock (above) + cooldown*	-0.01	+0.01	+0.14	-0.26
Vibration [per JPL Spec No. 30250B, 4.3.3.3 (a), Amendment No. 2]	-0.02	-0.01	+0.02	+0.16
Acceleration (14 g, static)	-0.05	-0.01	+0.06	+0.07

*Essentially, after one cooldown the RT and MU_{IA} values returned to their preshock values.

Table III. Mechanical and Performance Characteristics

Parameter	Result
Angular Momentum	$1 \times 10^5 \text{ g-cm}^2/\text{sec}$
Wheel Speed	24,000 rpm
Damping @ Operating Temperature	644 dyne-cm-sec
@ 50°F	2764 dyne-cm-sec
Operating Temperature	114.5°F
Gimbal Freedom	+0.55 deg -0.56 deg
Weight	0.997 lb
Length	3.096 in.
Diameter (excluding flange)	2.105 in.
Flange Diameter	2.24 in.
Spinmotor	
Power, Start	6.8 watts
Power, Run	3.5 watts
Torque Margin	5 volts (19%)
Run-up Time	15.7 sec
Run-down Time	56.7 sec
Pickoff	
Sensitivity	24.1 volts/rad
Null Voltage	1.2 mv
Torquer	
Scale Factor	356.085 deg/hr/ma
Linearity	+0.023% @ 0.24 deg/sec -0.026% @ 0.48 deg/sec +0.0018% @ 0.95 deg/sec
Stability	0.018%
Slew Rate Capability	>11,000 deg/hr
Temperature Sensitivity	0.57% (100°F to 130°F)
Hydrostatic Pump	
Frequency	499 Hz
Power	0.6 watt

Table IV. Performance Parameters

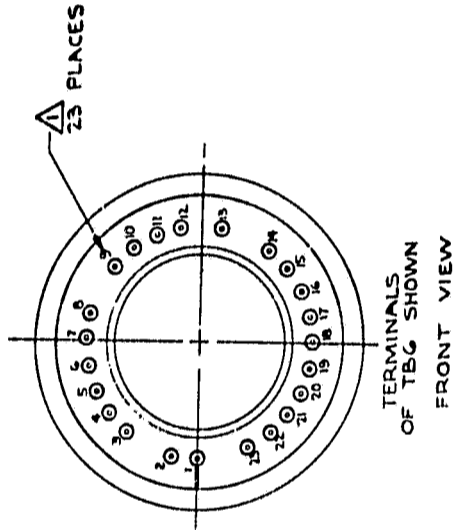
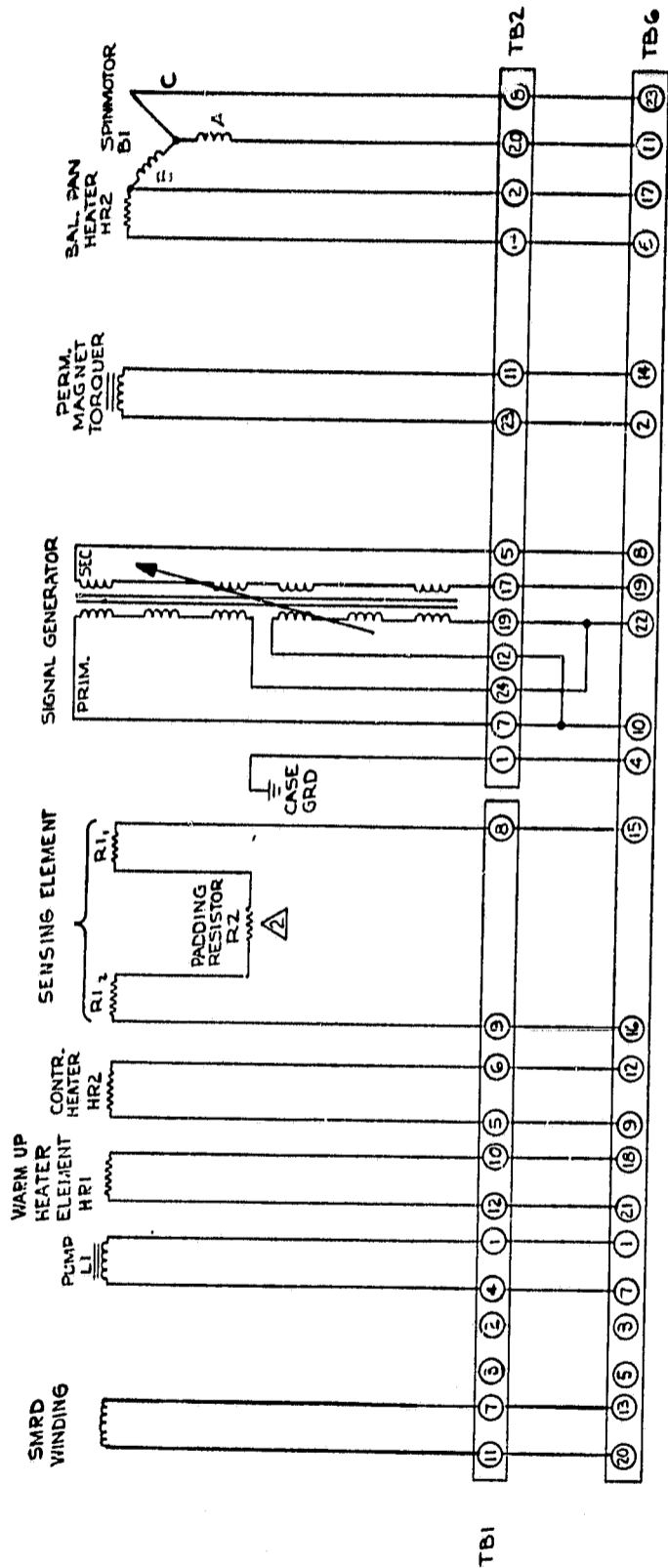
Parameter	Value
Fixed Torque (as shipped)	-0.158 deg/hr
MU _{IA} (as shipped)	+0.414 deg/hr/g
MU _{SRA} (as shipped)	+1.54 deg/hr/g
RMS Drift Stability	
OAV	0.041 deg/hr rms
IAV	0.070 deg/hr rms
Drift Stability (Cooldown)	
Fixed Torque	0.09 deg/hr rms
MU _{IA}	0.049 deg/hr rms
MU _{SRA}	0.064 deg/hr rms
Random Drift	
OAV (1σ)	0.005 deg/hr
IAV (1σ)	0.005 deg/hr
Elastic Restraint	-0.042 deg/hr/mr
Anisoelastic Coefficient	See Figure 3

Table V. Excitations Required

Signal Generator	
Voltage	10.5 volts rms
Frequency	7200 Hz
Spinmotor	
Start Voltage	26 volts rms - 2 Phase
Run Voltage	26 volts rms - 2 Phase
Frequency	800 Hz
Piezoelectric Pump	
Voltage	100 volts rms
Frequency	490 Hz
Heaters	
Warm up (55 watts)	120 volts max (ac or dc)
Control (10 watts)	40 volts max (ac or dc)
Sensor	10 ma max (ac or dc)

Table VI. Current Resistances and Inductances

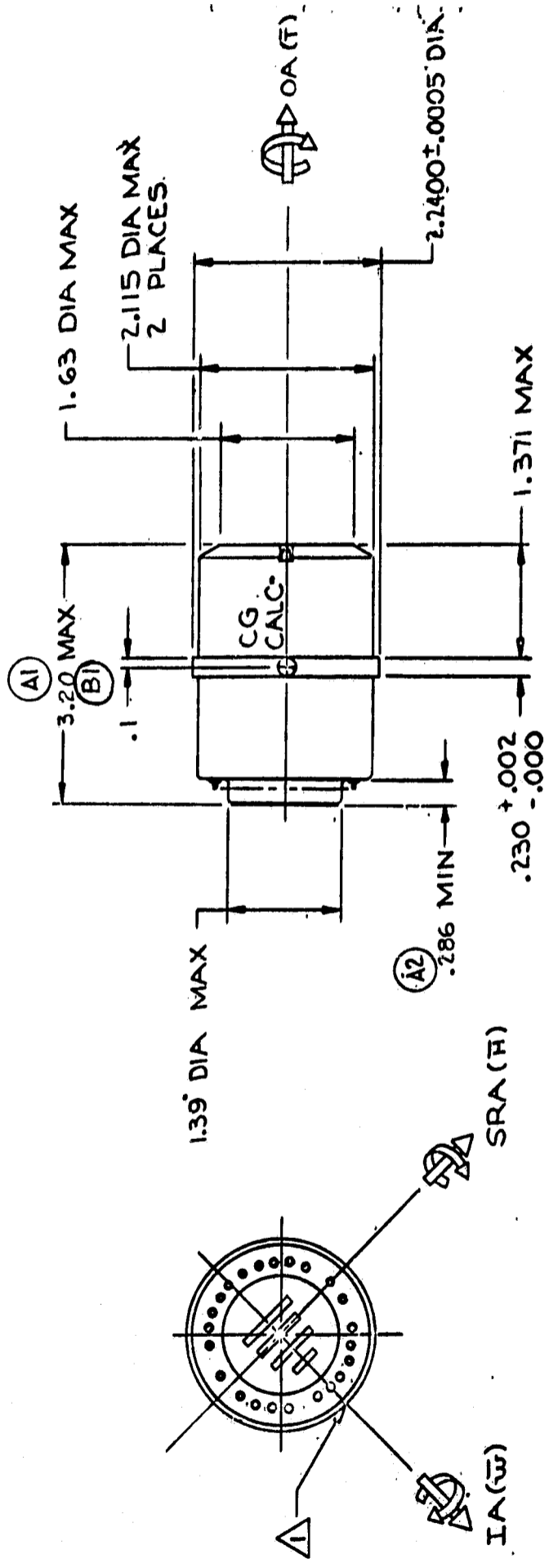
Circuit	Resistance @ 115°F (Ohms)	Inductance @ 115°F (mh)
Spinmotor		
ϕ A - C	36.95	--
ϕ B - C	35.88	--
Signal Generator		
Primary	30.59	2.0
Secondary	140.7	2.0
Torquer	161.8	3.44
Sensor	780.7	--
Heaters		
Warmup	278.5	--
Control	146.4	--
SMRD	751.0	--
Balance Pan	52.61	--
Torquer @ 70°F	149.2	3.40



△ RESISTANCE AS REQD

△ NUMBERS ARE FOR REF ONLY AND DO NOT APPEAR ON PART

Figure 1. Schematic Diagram



▲ SCRIBE MARK DESIGNATES POSITIVE
 IA LOCATION WITHIN ±1°

Figure 2. Installation Drawing

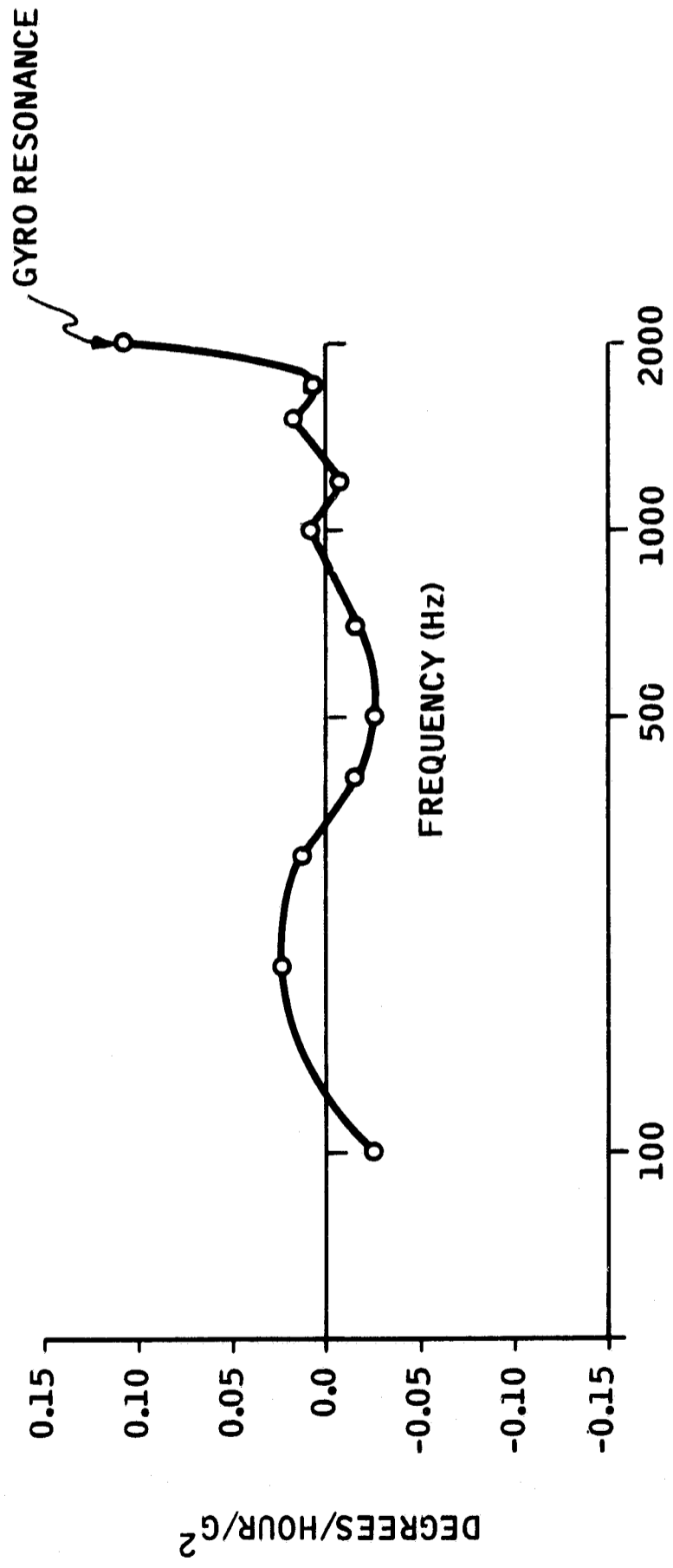


Figure 3. GG159E Anisoelectric Coefficient (100 Hz to 2000 Hz)

HISTORICAL PERSPECTIVE

This program was the logical extension of previous contracts, between JPL and Honeywell, which had developed the technology necessary to accomplish the objectives of this contract. These programs are historically accomplished as follows.

<u>Date</u>	<u>Technical Accomplishment</u>	<u>Work Performed Under</u>
July 1964	Study program to improve acceleration, vibration, and shock capability of the GG159C GBSM	JPL Contract 950604
December 1964	High rate torquer development study	JPL Contract 950604 (Mod. 3)
January 1965	High-g gyro completed (GG159C7)	JPL Contract 950604 (Mod. 2)
April 1965	High-frequency pump study	JPL Contract 950604 (Mod. 3)
June 1965	Sterilizable gyro completed (GG159D1)	JPL Contract 950769
December 1965	Sterilizable High-g gyro completed (GG159D2)	JPL Contract 951139
April 1966	High rate torquer fabricated	Honeywell funded
June 1966	"Umbrella-style" spinmotor fabricated	Honeywell funded
September 1968	Sterilizable, high-g, low-power gyro shipped (GG159E)	JPL Contract 951559

ORGANIZATION OF REPORT

Notwithstanding the groundwork which had been done on the previous programs, much design effort, evaluation, and analysis remained necessary on the present program. The results of this effort are presented chronologically according to the following breakdown:

- Section II - High-g Capability -- Low-Power Motor Development
- Section III - High-Frequency Pump Development
- Section IV - Sterilization

Some conclusions based on the results of the program are presented in Section V.

SECTION II
HIGH-G CAPABILITY --
LOW-POWER MOTOR DEVELOPMENT

Work to increase the g capability of the Gas Bearing Spinmotor (GBSM) began with JPL Contract 950604. The work was performed in two phases. Phase I determined the existing capability of the GG159C style motor, and Phase II increased the GBSM capability to meet the JPL shock (200 g) and random vibration (25 g rms) requirements. The results of this program were then incorporated into the build of the GG159C7 gyro and later into the GG159D2 gyro. The resultant design, however, had the disadvantage of relatively high spinmotor power requirements and dual-voltage start/run operation. A major design goal of this present program then was to combine the high-g capability with low-power and single-volt start/run operation. This was accomplished by utilizing the low-power, "umbrella-style" spinmotor design from the GG334 gyro shown in Figure 4.

GAS BEARING SPINMOTOR (GBSM) DESIGN -- FIRST ITERATION

The new gas bearing spinmotor geometry was set principally by the shock and power requirements. From squeeze-film considerations, short-duration shock capability is primarily a function of bearing area. This holds for either thrust or journal bearings. Power is a function of bearing drag, which in turn is proportional to the thrust (OD)⁴, journal (OD)³, and journal length. Table VII shows a comparison of these parameters for the GG159C, D, and E spinmotors.

With these relationships in mind, it can be seen why the earlier gyros required high power. The minimum journal OD was set in the GG159C and D, not by gas bearing considerations, but by the minimum OD of the stator. Since the journal OD was not optimized, the thrust bearing design could not be optimized. The GG159C and D thrust area was 0.855 square inch and was found to possess g capability in excess of 300 g. The journal area had 200-g capability with an area of 0.49 square inch. From this, an optimum value of 0.5 square inch was selected for both the thrust and journal bearings in the GG159E.

Due to the short duration of the shock, the load carrying capability is mainly obtained at frequencies higher than 500 Hz. Figures 5 and 6 show that increased support was obtained in both GG159 and GG334 style spinmotors by reducing the number of patterns on the thrust pad from 18 to 6. This is in addition to the load carrying capability obtained from squeeze-film support. From this information, the initial GG159E spinmotor was designed utilizing the six-pattern thrust pad similar to the GG334.

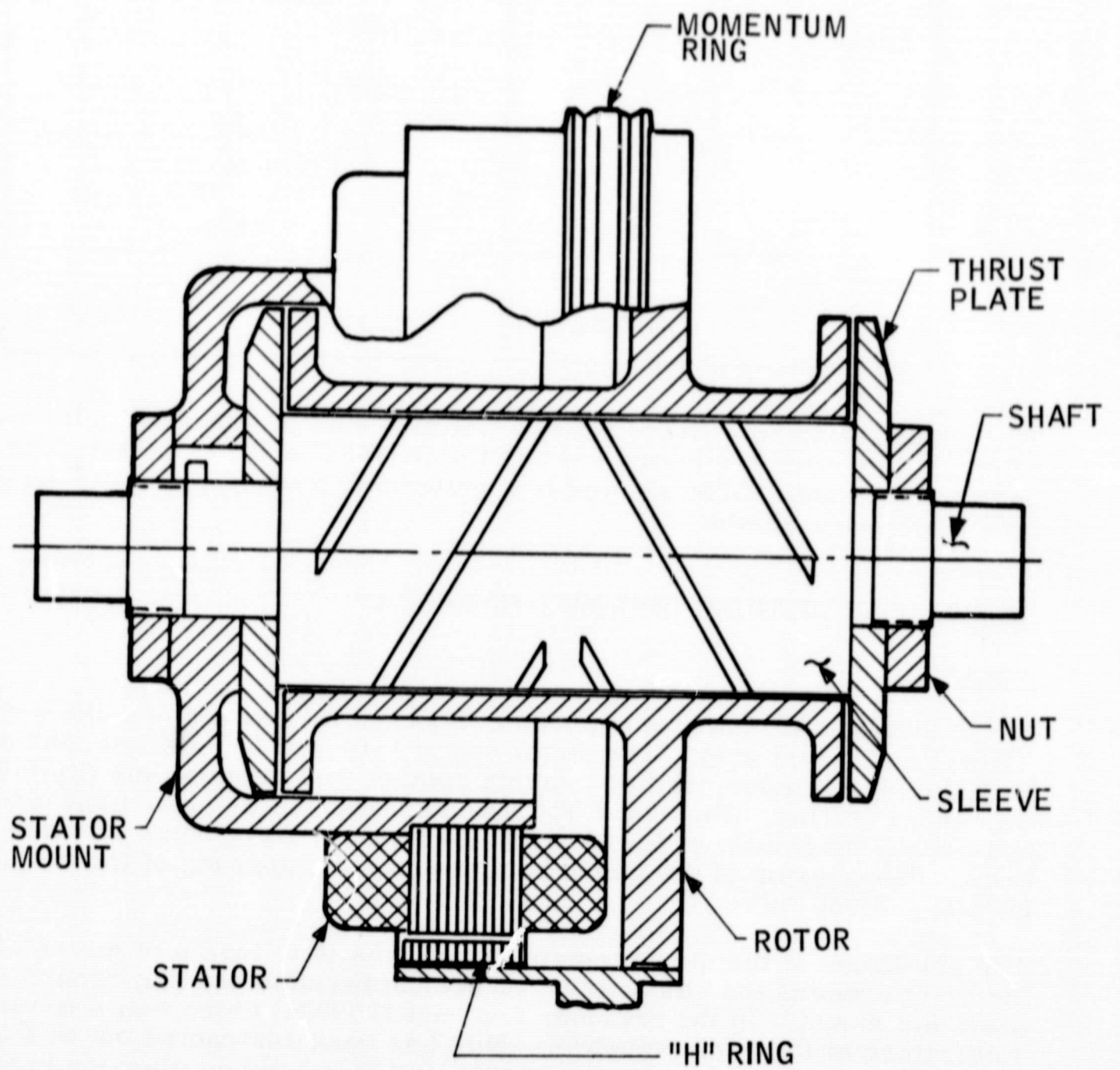


Figure 4. Low-Power Spinmotor Configuration

Table VII. Area and Drag Parameters

		GG159 C and D	GG159E
Thrust	Area	0.855	0.5
	OD	0.94	0.69
	(OD) ⁴	0.77	0.23
Journal	Area	0.49	0.5
	OD	0.58	0.4
	(OD) ³ XL	0.19	0.05

The journal bearing utilized a three-pattern shaft to suppress half-speed whirl rather than the lobing used in the GG159 C and D. Independent work on the GG334 and GG258 showed that patterning was superior to lobing for small-diameter shafts.

INITIAL GAS BEARING SPINMOTOR TESTS

Shock

A motor was built and was exposed to shock levels as high as 230 g on the journal and thrust axis. The shock was a 1.0- and 1.5-millisecond duration half sine shock pulse, and no bearing contact was made at any time during this shock testing. Figures 7 and 8 show the shock displacement plotted against the magnitude of the shock pulse with the waveforms at various positions. The ringing of the gas bearing caused the upswing of the displacement versus g-level curve.

The amplitude of the displacement waveforms is in terms of microinches, and the level exceeds the gas bearing clearance because bending occurs in the shaft and mount. In the previous contract (950604) there was a fixture error determined of 0.14 microinch/g. This has been subtracted out of Figures 7 and 8 and the remaining displacements are then bending plus gas bearing displacement. The positive determination of no bearing contact is made by observing the lissajous pattern of the motor TIR and motor voltage. A minute change in the pattern (i. e., a loss of synchronism between physical rotor rotation and electrical field rotation) can be easily observed to indicate bearing contact.

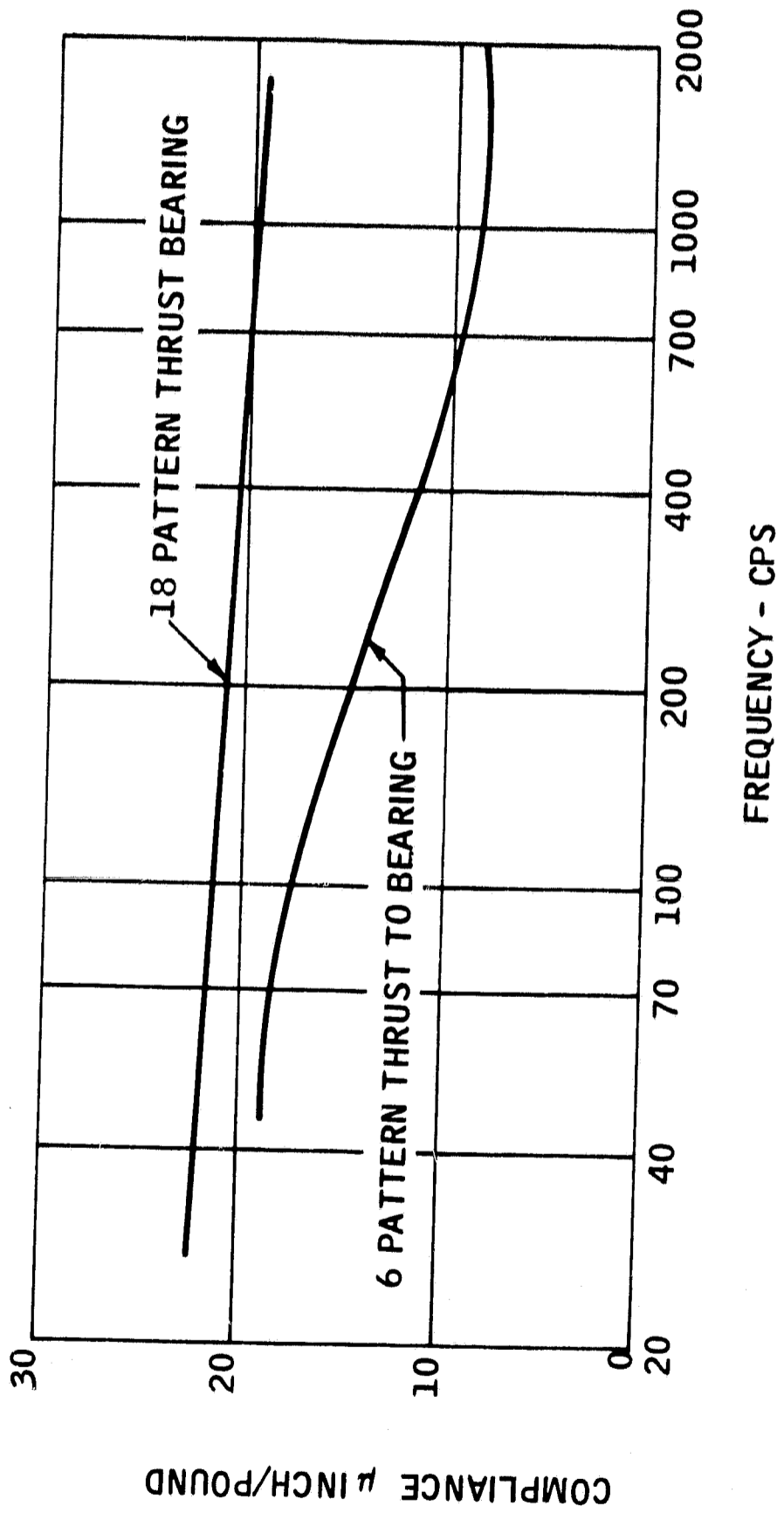


Figure 5. GG159 Thrust Bearing Frequency Response

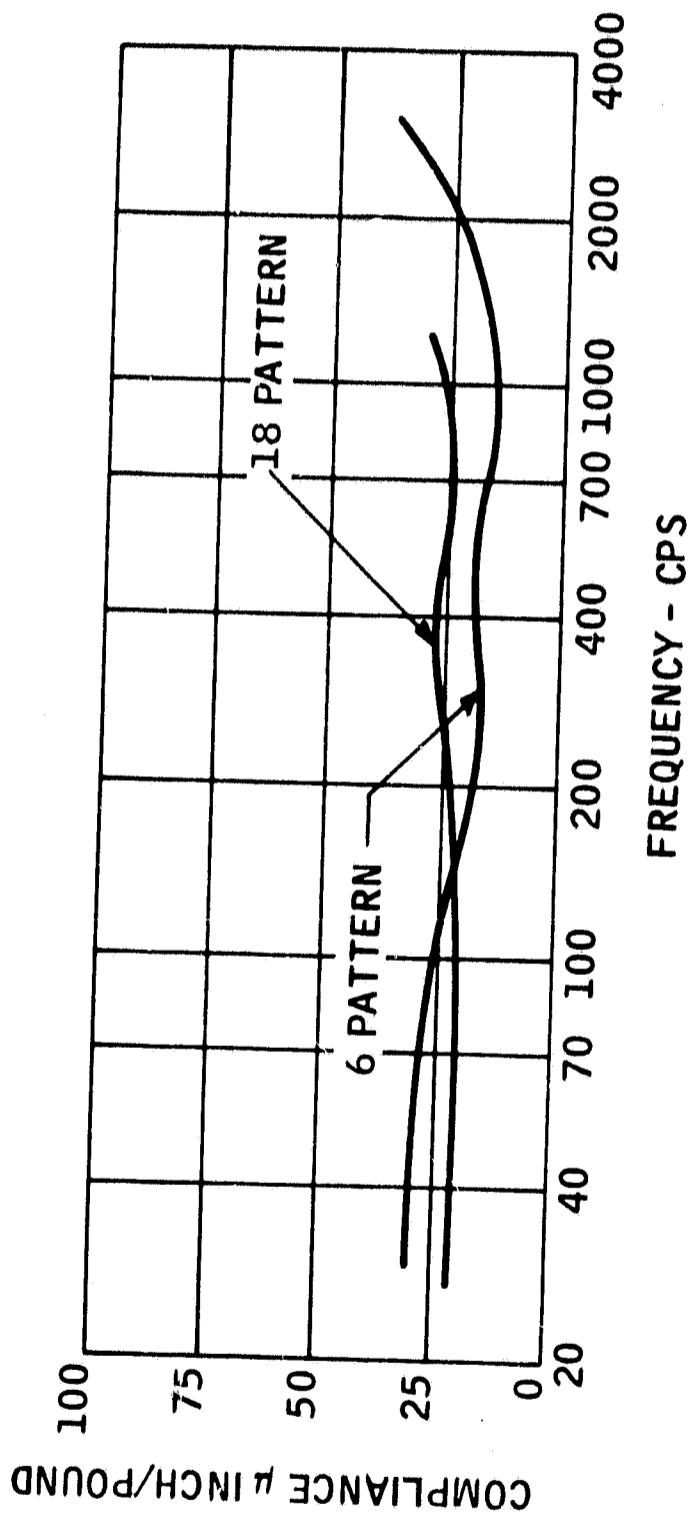


Figure 6. GG334 Thrust Bearing Frequency Response

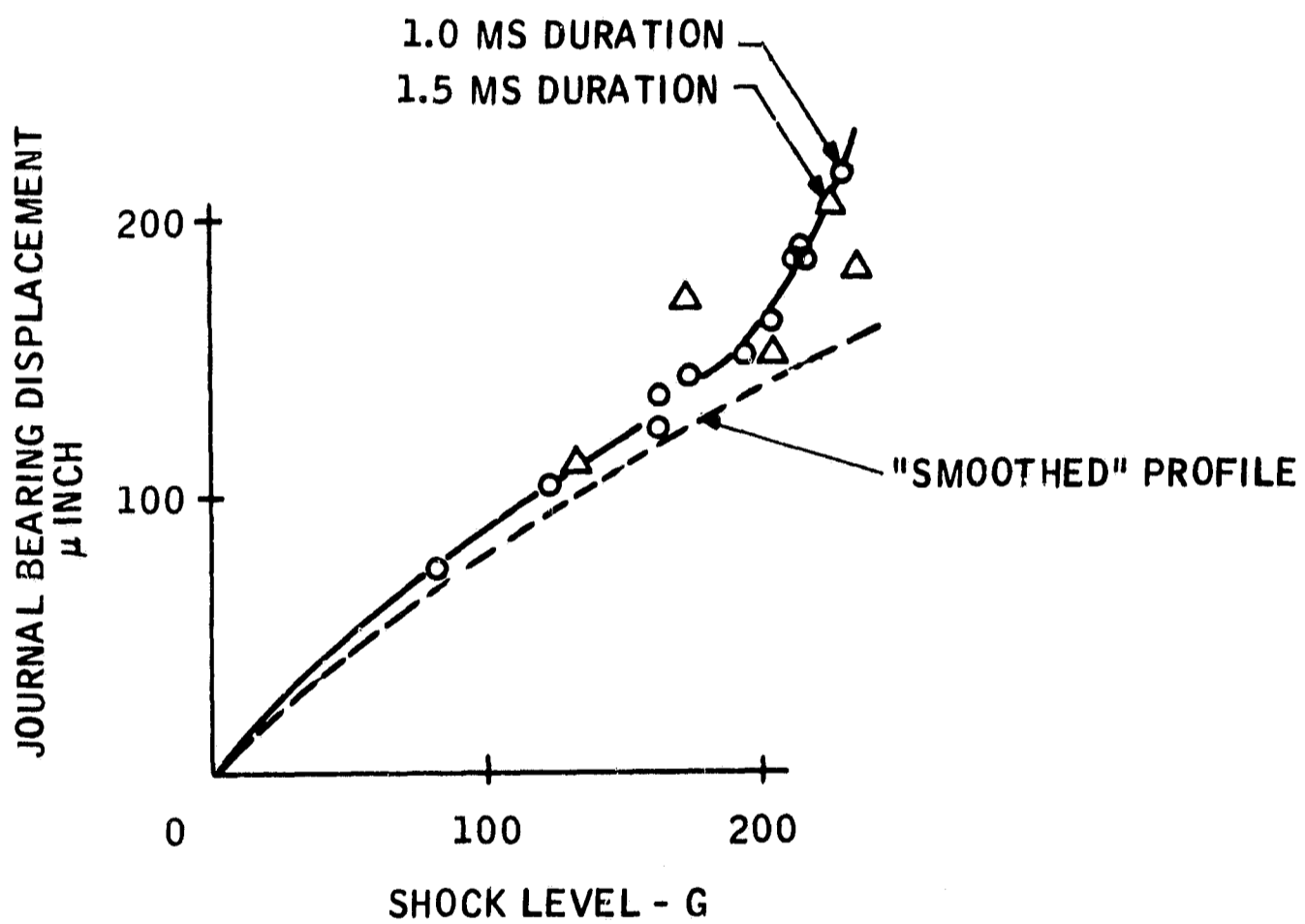


Figure 7. GG159E Bearing Displacement versus Shock Magnitude

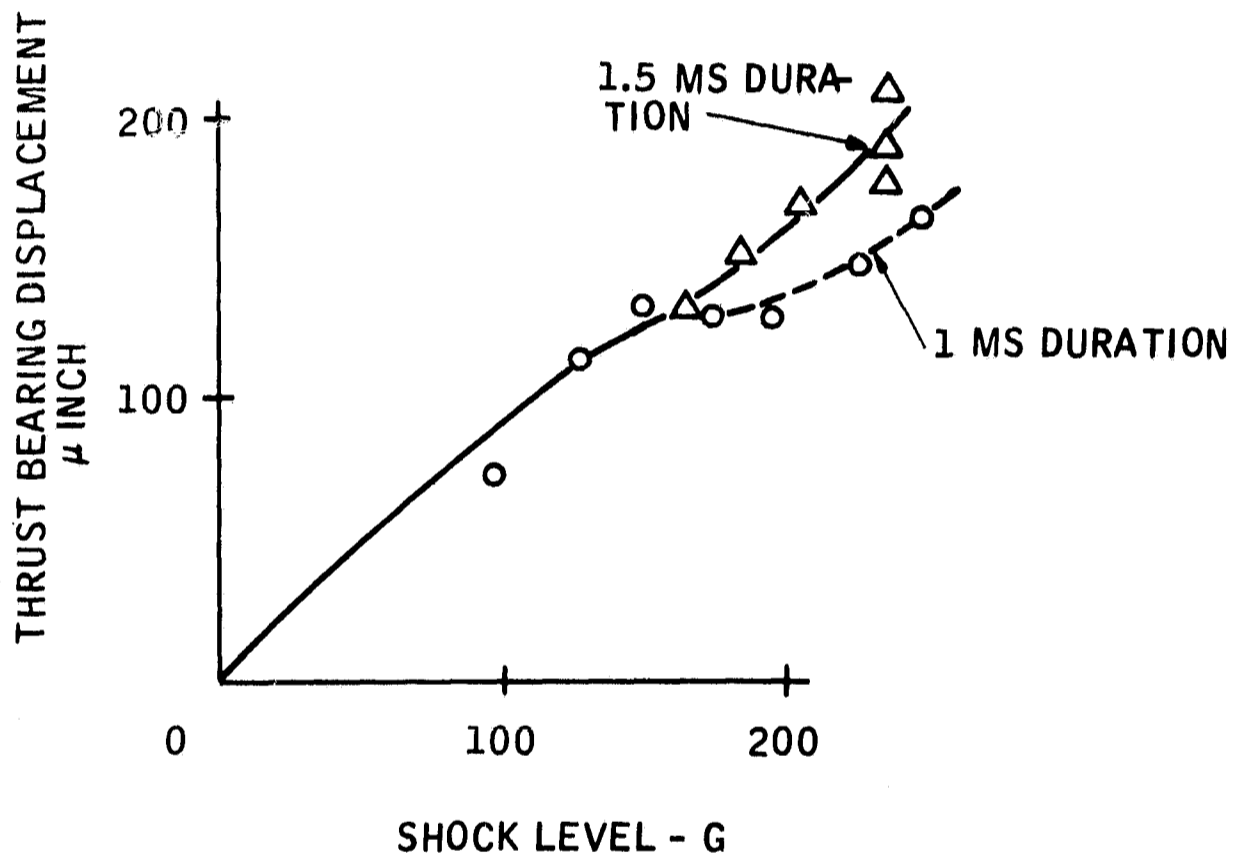


Figure 8. GG159E Bearing Displacement versus Shock Magnitude

Random Noise

An exposure of the GG159E gas bearing spinmotor to random noise as specified in the JPL Spec No. 30250B 4.3.3.3 (a) modified by Amendment No. 2 was successful. No bearing contact was made, and the displacements were linear and were less than encountered in the shock testing. The lack of bearing contact was determined again by observing the synchronism of displacement and motor voltage.

FINAL GBSM DESIGN

As testing continued on the spinmotor and the gyro, the lockup and contamination problems described in Section IV necessitated minor changes in geometry and magnetics. The nonsymmetrical journal pattern which solved the moisture lockup problem reduced the thrust bearing g capability by 20 g to 40 g. This was corrected by further experiments which led to a final thrust plate configuration utilizing 3 patterns rather than 6.

Electrical and Magnetics Design

Spinmotor power is as dependent upon a good magnetic and electrical configuration as upon minimized mechanical power in the gas bearing. The basic magnetic and stator design was adapted from the GG334 spinmotor for use on this program.

The canned stator and slot bridge, which were added to eliminate the particulate contamination discussed in Section IV, affected power and warranted a series of magnetic tests to be conducted with the various combinations shown in Table VIII. Design consideration was also given at this time to a solid liner for the laminated P-6 hysteresis ring.

These tests showed that adding the slot bridge and stator cans and reducing the air gap to 0.002 inch produced a motor with reasonable sync and start margins with acceptable power consumption. Lining the hysteresis ring was not desirable from a power standpoint and was not incorporated.

GYRO TEST RESULTS

Shock, vibration, and acceleration test results were accomplished on the preliminary gyro build with the test results shown in Table III. Those results verify that, besides survival of the spinmotor, the gyro performance is not significantly disturbed by such environments.

Results which track the spinmotor performance over sterilization are presented in Tables XI and XII. Again, no deterioration may be seen.

Table VIII. GBSM Magnetics Test Results

Canned stator - standard H-ring rotor		
air gap = 0.002 in.	Power	3.0 watts
	Sync Margin	7.0 volts
	Start Margin	6.0 volts
air gap = 0.004 in.	Power	4.2 watts
	Sync Margin	6.0 volts
	Start Margin	6.0 volts
Canned stator - lined H-ring rotor		
air gap = 0.001 in.	Power	3.6 watts
	Sync Margin	2.0 volts
	Start Margin	4.5 volts
air gap = 0.002 in.	Power	3.9 watts
	Sync Margin	3.0 volts
	Start Margin	5.0 volts
air gap = 0.004 in.	Power	4.0 watts
	Sync Margin	4.0 volts
	Start Margin	6.0 volts

While the final gyro spinmotor power of approximately 3.5 watts was well within the 4.0-watt requirement of this contract, a test result from another program is worth noting. The exact spinmotor design used in the GG159E, but with a minor windings change to further reduce power, was built into GG334S, SN B1 (JPL Contract 951529). The motor required 2.5 watts running power and demonstrates the possibility of further power savings if ever required. The decision to remain at 3.5 watts was based on building in the maximum motor torque margin consistent with the program requirements for power.

SECTION III HIGH-FREQUENCY PUMP

The high-frequency pump development program which was initially started under JPL Contract 950604 has been continued under this contract. Whereas the emphasis on the previous development program was to demonstrate the feasibility of the high-frequency pump concept, the object of the current effort was to develop the necessary hardware to implement the high-frequency pump into the GG159E gyro.

DETERMINATION OF A MOUNTING SCHEME

The following methods of mounting the pump plate were designated and tested:

- Lead-coated aluminum V seals
- Solid spacers
- O-Rings

The test was implemented with a manometer and flow meter, the excitation frequency was variable, and a valve allowed flow control.

The results of these tests are shown in Table IX, where the aluminum V seals were selected as the best method of holding the piezo electric pumping assembly.

CARTRIDGE PUMP DESIGN

A cartridge-type, high-frequency pump assembly was first designed (Figure 9). The pump assembly was purposely designed to fit into a GG159D2 case and to utilize the same plumbing, gyro mounting, and seals. The lead-coated aluminum V seals were chosen for this design because of the high-pressure flow output obtained from the initial tests and of the high probability of being able to withstand sterilization temperatures without damaging the bender plate and/or altering the pumping characteristics.

The basic parts of the pump assembly were the pump housing, rectifier plate, lead-coated aluminum V seals, rectifier retaining ring, and piezo plate assembly.

The piezo plates making up the piezo plate assembly were zirconate ceramic. The plates were coated with sputtered gold to create the conductive surface which was approximately 50 angstroms thick. The plates were axially polarized and epoxied together so that the positive side on one plate was

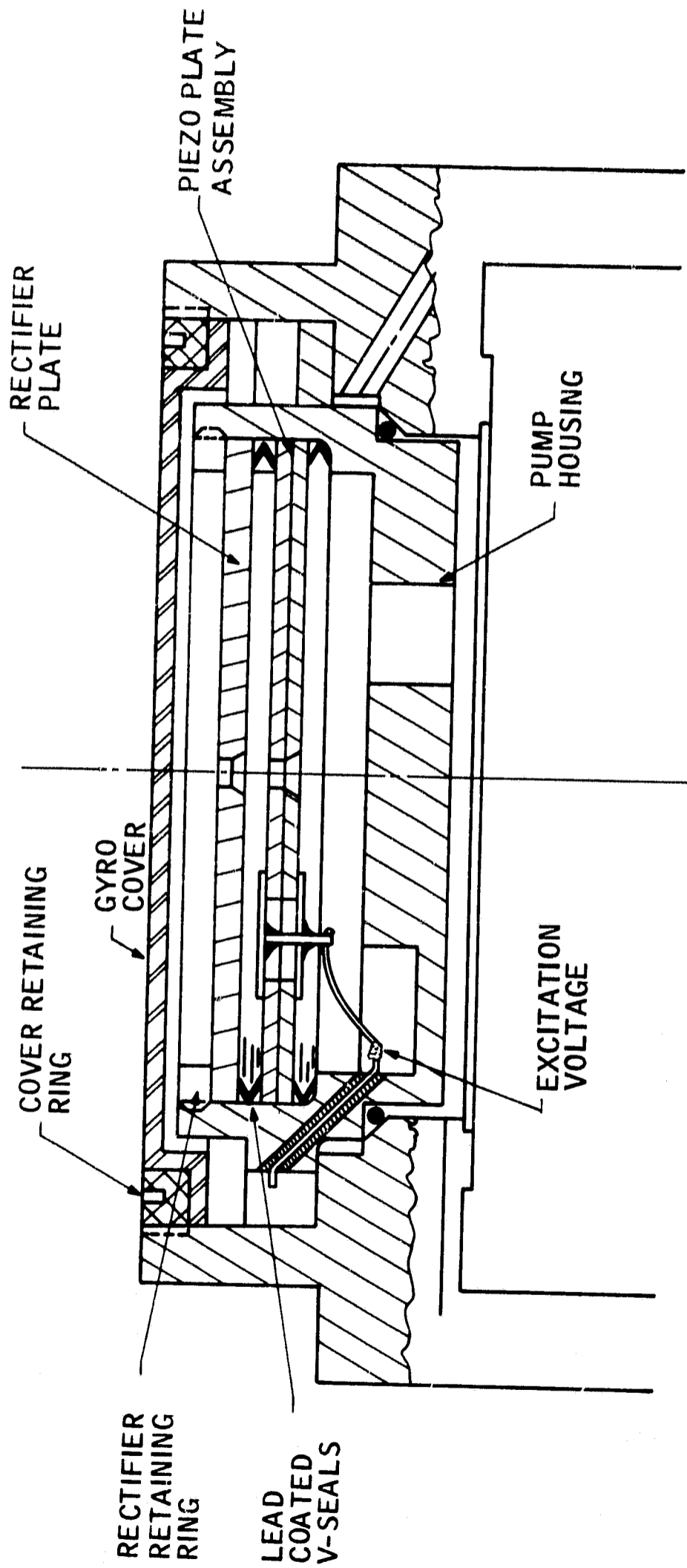


Figure 9. High-Frequency Pump Layout

Table IX. Results of Three High-Frequency Pump Mounting Schemes

	Advantage	Disadvantage
V-seals	<ul style="list-style-type: none"> 1) Simple construction 2) Highest pressure and flow 3) Bender plate clamping force is virtually constant with temperature 4) Mounting system is not degraded after exposure to sterilization temperatures 	<ul style="list-style-type: none"> 1) The most frequency sensitive
Solid Spacer	<ul style="list-style-type: none"> 1) Simple construction 	<ul style="list-style-type: none"> 1) Bender plate clamping force would be sensitive to temperature 2) Pressure-flow output curve is erratic
O-Rings	<ul style="list-style-type: none"> 1) Simple construction 	<ul style="list-style-type: none"> 1) Bender plate clamping force would be sensitive to temperature 2) O-Ring may take a "set" change output characteristics 3) Pressure-flow output is less than with V-seals

epoxied with conductive epoxy to the negative side of the adjacent plate. After the terminals were attached and excited with an a-c voltage, the assembly would bend like a bimetal structure undergoing a cyclical temperature change. The pumping orifice was ground directly into the bender assembly. This piezo pumping plate assembly is shown in Figure 10.

When the cartridge-type, high-frequency pump was completed, the alkane 695 damping fluid was received from the vendor. Tests were then run on the pump mounted in a gyro case to determine the resonant frequency as well as the pressure and flow output versus frequency. The results are plotted in Figure 11.

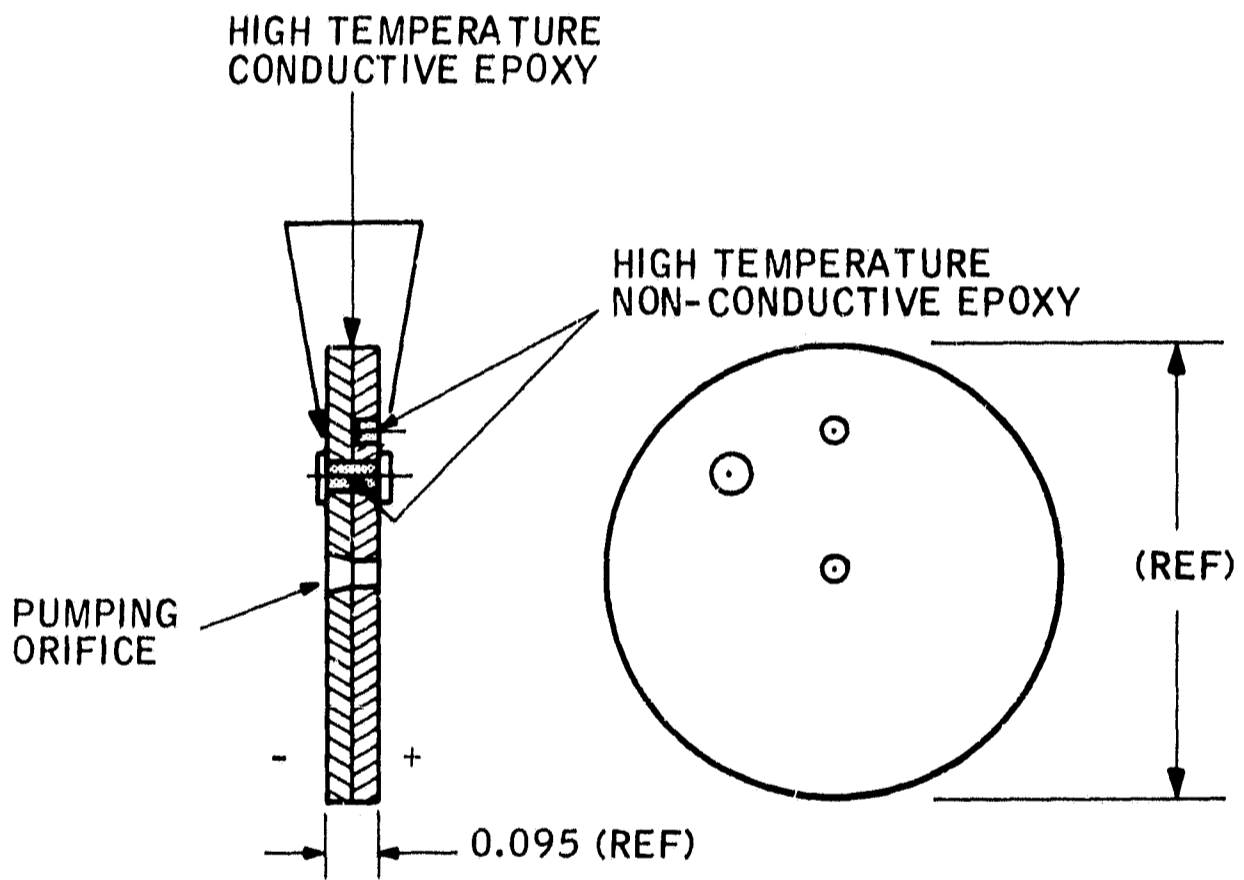


Figure 10. Piezo Pumping Plate Assembly

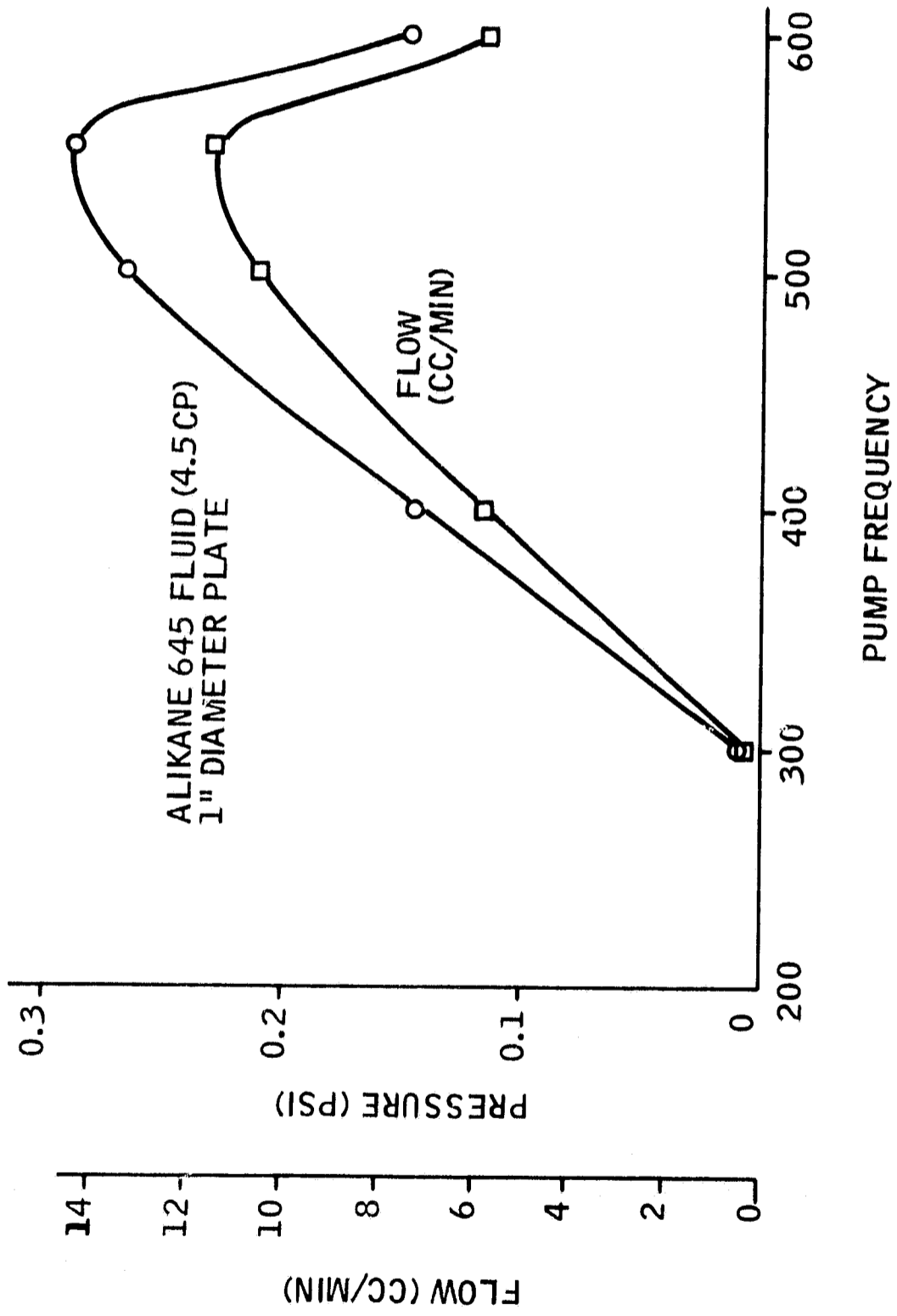


Figure 11. Piezo Pump Pressure and Flow versus Frequency

As can be seen from the curve, the peak pressure and flow output occurred at about 540 Hz, which was well above the anticipated design point of 400 Hz. This assembly was exposed to 300°F for 100 hours at this time, and no change in the output was observed.

Since the cartridge assembly was desirable for dummy gyro assemblies and tests at this time, the resonant frequency was not thought to be the immediate problem and was left for future reconsideration. Seven variables were recognized at this time to be involved in the resonance of this system. These variables were:

- Plate spacing
- Rectifier compliance
- Gyro cover spacing and compliance
- Fluid density
- Fluid viscosity
- Plate diameters
- Bender plate mass

Dummy Gyro

The viscosity of the purchased alkane 695 fluid was low by 30 percent, and the density was low by 3 percent as compared with the purchase specification. This created pump support and flotation problems on a GG159 dummy gyro (no spin-motor) evaluation of the high-frequency pump. Marginal support was obtained, and further evaluation with a fluid with proper parameters was required to assess the true capability of the pump.

An additional problem of a 2000-micron vapor pressure made the gyro filling extremely difficult. Elimination of entrapped gas was required for proper operation of the high-frequency pump. It was estimated that a maximum of 200-micron vacuum pumpdown during fill would be required to obtain the most efficient pump operation. A search for a better fluid was then undertaken.

SUSPENSION FLUID SEARCH

Inquiries were directed to prospective vendors using the following fluid-property requirements:

- 1) Density: 1.87 gm/cm³ minimum, at 115°F
- 2) Viscosity: 2-centipoise minimum at 130°F and 12 centipoise maximum at 50°F
- 3) If no fluid fulfilled (1) and (2), inquiry was made on the basis of maximum 115°F density value with viscosity of 12 centipoise or on the basis of 50°F and 130°F viscosity values for any available fluid with a density of 1.83 gm/cm³ at 115°F
- 4) Minimum vapor pressure

The following vendors were contacted for availability of fluids:

- Petroleum Chemical Division, E.I. DuPont
- Freon Products Division, E.I. DuPont
- Chemical Division - Minnesota Mining and Manufacturing Co.
- Chemical Research and Development Center, FMC Corporation
- Halocarbon Products Corporation
- Hooker Chemical Company

No completely satisfactory fluid (requirements 1 and 2) or alternate was proposed by the vendors. Inasmuch as the high-density and low-viscosity specifications were not compatible, the best fluid noted was the FC-43 monomer fluorolub fluid which had the following pertinent properties:

- Density: 1.844 at 115°F
- Viscosity: 7.5 centipoises, 50°F
2.71 centipoises, 115°F
2.24 centipoises, 130°F
- Stability: Very Good
- Excellent material compatibility: Distills at constant composition
- Vapor Pressure: 1000 microns at 100°F
300 microns at 77°F

SUSPENSION DAMPING

The gimbal suspension damping over the 50°F to 130°F temperature range was calculated assuming FC-43 fluid and is shown in Figure 12. The damping sensitivity was slightly less than that which would result from use of the alkane 695 fluid; the values met the sterilizable gyro specifications.

GYRO REDESIGN

With the use of FC-43 fluid, a gyro redesign was necessary which allowed flotation at 115°F by increasing the gimbal diameter. To accommodate the high-frequency pump operations at 400 Hz, the cartridge assembly technique was dropped and the pump diameter was increased. The result of the pump diameter increase and the gimbal diameter increase was a gyro which was intended to meet contractual requirements of

- Size - external gyro dimensions
- Temperature - 50°F to 130°F
- g capability - random and shock requirements
- Pump excitation frequency - 400 Hz sine
- Damping - 500 dyne-cm-sec at 115°F, 1800 max at 50°F to 130°F

SUSPENSION-FLUID GAS-CONTENT

An extensive test of the high-frequency pump was conducted with the best pump hardware and gyro fill procedures using the FC-43 fluid and a dummy gyro (no spinmotor). The life of this dummy gyro was three days, at which time the performance (drift) degraded significantly. This type of degradation was observed at shorter intervals on other assemblies and was identified as a bubble developing between the piezo disk assembly and the rectifier plate. This short life was studied in a test which identified the pump life as a function of suspension fluid dissolved air content.

A life test was then assembled using a high-frequency pump assembly similar to those used on Contract 950604 modification 3 and using the FC-43 fluid. The difference between this test and those on the previous contract was the addition of a "degassing station" shown in Figure 13. Degassing of the fluid occurred at the pressure imposed on the surface of the fluid at the "degassing station". As there were small leaks in the system, the pressure P_g (Figure 13) increased as the gas entered the system, and the system needed to be pumped down about once a week to provide ± 1 psi regulation. For this test, P_g was

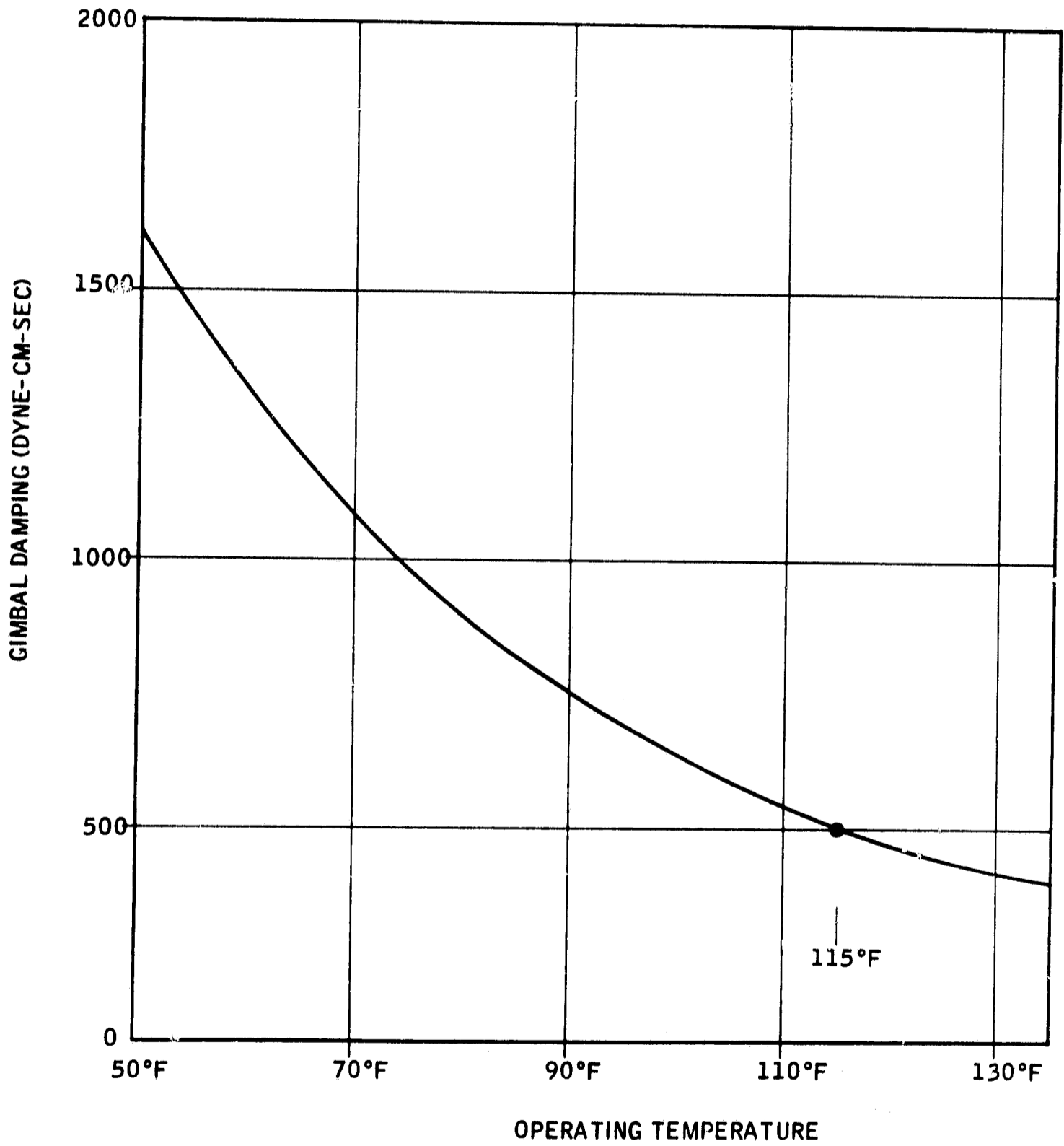


Figure 12. Gimbal Suspension Damping over the 50°F to 130°F Range

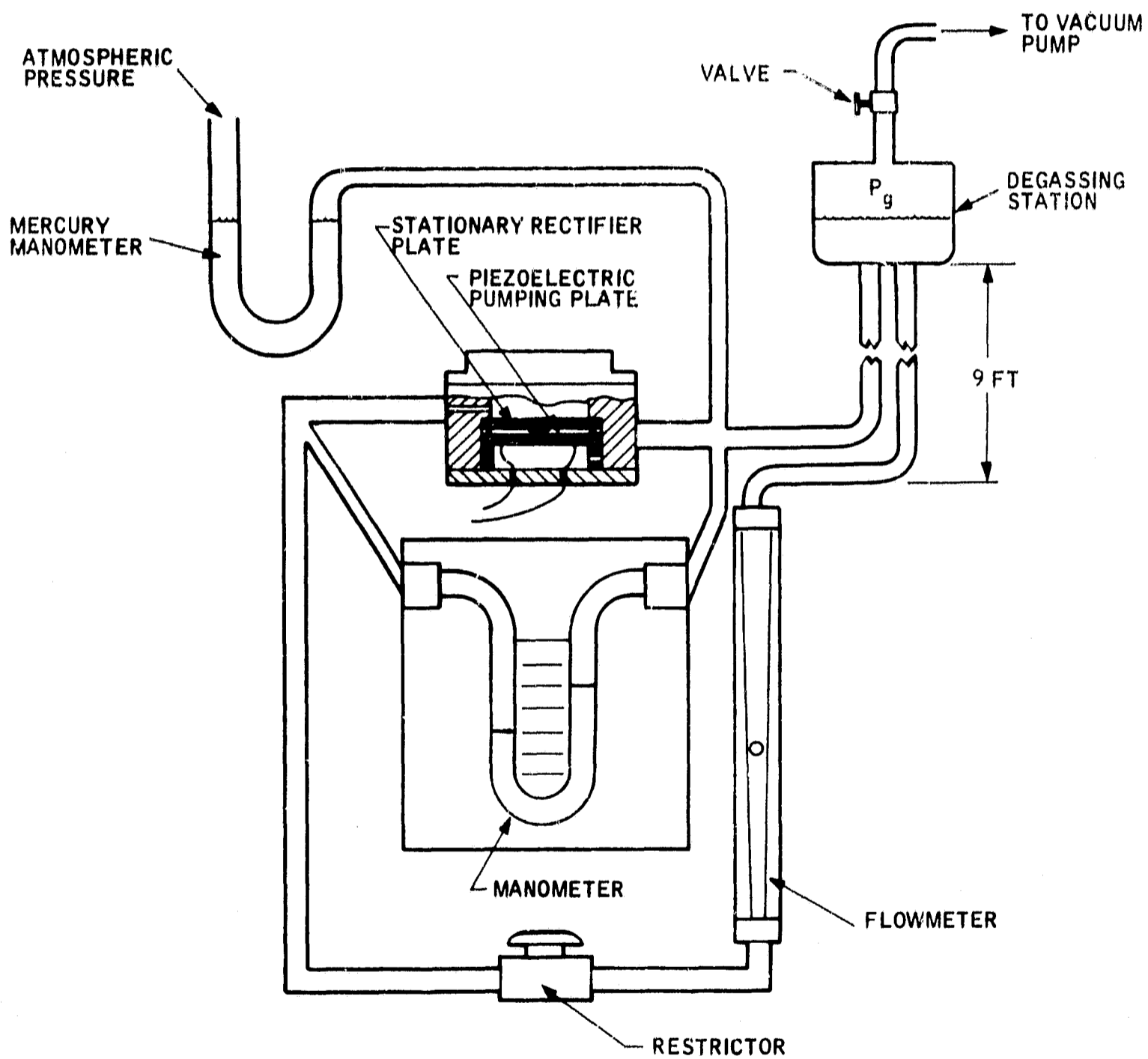


Figure 13. Piezoelectric Pump Life Test

set at 7.5 psia to provide 15 psia at the pump (nine feet of FC-43 is a head of 7.5 psi). This pressure differential was determined to be sufficient to allow the pump to operate for three months on a continuing life test.

When the pressure head was decreased to 2.5 feet and P_g was increased to 13 psia, the pump began to develop symptoms similar to those when gas bubbles were observed in the pump; i. e. the pressure output would drop with time.

The pump life test was terminated at 3.5 months with no noticeable changes in performance. The test was stopped because fluid was being lost at an increasing rate through the vacuum pump and was causing loss of vacuum in the system. The 3.5-month life was 15,000 times longer than tests performed in fluid which was exposed to 15 psia instead of the reduced pressure exposure of this life test at 7.5 psia. This was sufficient to identify the saturated gas level as the life reducing factor in the high-frequency pump.

TEST RESULTS IN THE GYRO

The final design of the pump using processing which reduced the saturated gas in the gyro was incorporated into the gyro design and was used successfully in two builds of the same hardware. The first (preliminary) build was carried out primarily to verify the pump design, knowing that the unit would have to be rebuilt to correct the spinmotor contamination discussed in Section IV. The piezo pump operated successfully during the life of the preliminary gyro build (420 hours), demonstrating proper support capability during shock, acceleration, vibration, and rate testing. Sterilization testing was not successful because of the limited bellows capacity discussed below. A change in the excitation frequency necessary to excite the pump, from 470 Hz to 400 Hz, occurred early in the history of this device. Subassembly tests run after the unit was torn down indicated that the cause of this frequency change was marginal preload on the V-rings. The tests showed that the assembly, when torqued as prescribed for the dummy gyro build, would loosen-up over temperature cycling. This loosening could in turn reduce the preload on the V-rings and eventually cause a change in the resonant frequency. Further testing showed that dimensional stability and a stable resonant frequency were obtained by increasing the prescribed torque valve and by stabilizing the assembly with temperature cycling. This procedure, however, resulted in a 490 Hz operation frequency.

The pump assembly in the final device showed perfectly stable operation throughout the test program, which included the sterilization cycling. Final test results on the pump are presented below.

- Pump power - 0.6 watt
- Operating frequency - 490 Hz
- Operating Life (as shipped) - 585 hours

SECTION IV STERILIZATION CAPABILITY

Development of sterilization capability in a gyro began with JPL Contract 950769. This work included extensive design study and testing to determine which materials and subassemblies would withstand sterilization cycling to a temperature of 300°F. Such problems, for example, as the corrosive properties of the damping fluid, epoxy strength, absorption rates of materials, and creep and magnetic stability at sterilization temperatures were investigated and resolved. These efforts culminated in the GG159D1 gyro which successfully withstood exposure to sterilization and were readily transferred to the later GG159D2 gyro which integrated sterilization and high-g capability.

The low-power spinmotor and high-frequency pump requirements necessitated some further design investigation and testing during the present program. These are explained in the following paragraphs.

SPINMOTOR MATERIALS

The low-power spinmotor configuration (Figure 4) used the materials shown in Table X. These materials were used in the GG159D2 gyro with the exception of the hysteresis ring, beryllium, and stainless steel. The item of greatest concern, the laminated hysteresis ring, was tested, and the ring held up under shock and sterilization with no visible degradation.

Table X. Materials in GBSM

Materials	Part
High-density alumina ceramic	motor and shaft sleeve
High-temperature epoxies	joints
High-temperature solder	electrical connection
Instrument grade beryllium	stator mount
303 stainless steel	nuts
Iron cobalt alloy (VA-Permendur)	stator laminations
Iron cobalt alloy (GE P6 alloy)	hysteresis ring laminations
High-density tungsten alloy	momentum ring
Zirconium alloy	shaft

LOCKUP

Early testing of the low-power spinmotor revealed an inability to restart the motor when it had been stopped after continuous running for periods between 10 and 100 hours. Moisture in the gimbal parts evaporated into the gimbal atmosphere and then was pumped into the gas bearing where it condensed. This condensation allowed the rotor to wring to the shaft when the motor slowed down and the gas bearing clearance approached zero. The point of wringing-in was indicated by an abrupt stopping of the rotor on rundown. The motor could be restarted if sufficient time (several days) was allowed for the water to evaporate. The starting voltages then quickly returned to original values with a few quick starts and stops. Running the motor for a few hours would repeat the cycle.

Drying the gas with a molecular sieve-type drying agent, combined with piece-part drying before assembly, extended the life of this motor but would not prevent the lockup from eventually occurring. It was shown that revised bearing patterning was necessary to accomplish the required life.

ASSYMETRICAL JOURNAL PATTERN

Moisture lockup was prevented by using a pattern which pumps gas through the bearing assembly, as opposed to the usual configuration which develops equal pressure at the ends of the journal bearing and which creates a high-pressure, zero flow condition. By pumping gas through the assembly of thrust and journal bearings, the moisture is carried away faster than it can condense.

Testing showed that the optimum pattern for preventing moisture lockup is the asymmetrical journal pattern. In this approach, one of the two journal patterns is made longer than the other. This asymmetry creates a pressure differential along the axial length of the journal bearing, resulting in axial gas flow.

The asymmetrical journal motor was tested under adverse moisture conditions with excellent results. After cleaning and assembly, the motor was mounted in a small, air-tight chamber and performance was monitored at the ambient relative humidity (RH) condition of 40 percent. Then, successive incremental amounts of water were added to bring the RH to 90 percent. No moisture lockup was observed. Table XI summarizes the results, which verified that the asymmetrical journal pattern successfully solved the moisture lockup problem.

OTHER VENTING APPROACHES

Two alternate methods were tested and were compared to the asymmetrical journal patterning at this time, thrust venting and center venting. Thrust venting, implemented by increasing the sealing band on one thrust plate, proved insufficient to remove moisture. One motor was built; this motor worked, but a second motor failed by locking up. Center venting, whereby gas is pumped through a hole in the center of the journal by the pressure developed in the thrust bearings, reduced the g-capability to the point that the 200-g shock was beyond the capability of the configuration.

Table XI. Moisture Lockup Sensitivity of Optimized Assymetrical Journal Design

Relative Humidity (%)	Running Hours	Motor Performance
40	1.0	No Lockup
50	3.0	No Lockup
60	2.0	No Lockup
70	2.0	No Lockup
80	2.0	No Lockup
90	2.0	No Lockup

PARTICULATE CONTAMINATION

Variability in starting voltage was noted during spinmotor testing during the preliminary gyro build. At about the same time, experience on another gas bearing program showed the possibility of organic vapor or particulate contamination causing lockup. Obviously, these mechanisms differed from the moisture mechanism, but the result was the same. Accordingly, an extensive program was launched to pinpoint and to remove any possible sources of contamination.

A series of analytical tools were developed to aid in pinpointing sources of contamination. These included

- Infrared Analysis -- A total of 14 organic materials were used (or could be used) in the GG159E gimbal assembly. Infrared maps were prepared for all 14 materials. With these maps, it was a simple matter to compare appropriate finger prints and to identify the contaminant.
- Ultraviolet-Fluorescence Analysis -- Since gas bearing contamination can sometimes be found in too small of a quantity for infrared analysis, ultraviolet fluorescence of the 14 organic materials was also prepared to form a standard for comparative checks.

- Mass Spectrometer Analysis -- Mass spectrometer analysis was used to sample gimbal fill gas for moisture content and for organic vapor constituents. A fixture was designed and built to permit direct gimbal gas sampling as shown in Figure 14. The gimbal is solidly clamped between the end nests with an O-ring primary seal. A wheel puller device was used to extract the fill plug, permitting the gimbal gas to enter the mass spectrometer chamber. The same fixture could also be used for gas chromatography cross checks.
- Gas Chromatograph Analysis -- Five materials were selected on the basis of quantity and of proximity to the motors for outgassing and dewpoint tests.
- Thermal Analysis Tests -- Thermal behavior of the 14 organic materials used for the above UV-fluorescence tests was also studied under a hot stage microscope capable of 350°C. Data from this analysis also enabled rapid identification of contaminant materials.

This effort resulted in specific identification of the contamination in the GG159E preliminary build. The resulting design change -- canning of the stator -- is discussed below. Other results were as follows:

- The lockup of specific gas bearing motors was due to organic-particulate contamination and not to vapor-condensed materials.
- The contamination was associated with bonding and encapsulating materials in the motor stator.
- Gas analysis of a sample filled gimbal showed the gas fill procedure used on the product line to be satisfactory.
- Materials presently used in spinmotor fabrication compare favorably with alternate materials tested either as used or with some additional processings. No material changes were implemented.
- Water vapor and organic outgassing tests verified the original assumption that these phenomena would be much more prevalent at sterilization temperature. As a result, special vacuum-bake processes were initiated as a prevention.

STATOR CANNING

A detailed visual examination of the gas bearing surfaces after preliminary build of the unit disclosed that a deposit had accumulated to form an annular ring on the thrust plate near the intersection of the thrust and journal bearings. Similar, though smaller, deposits were noted on the rotor in the same region. A 425X magnification of this ring is presented in Figure 15.

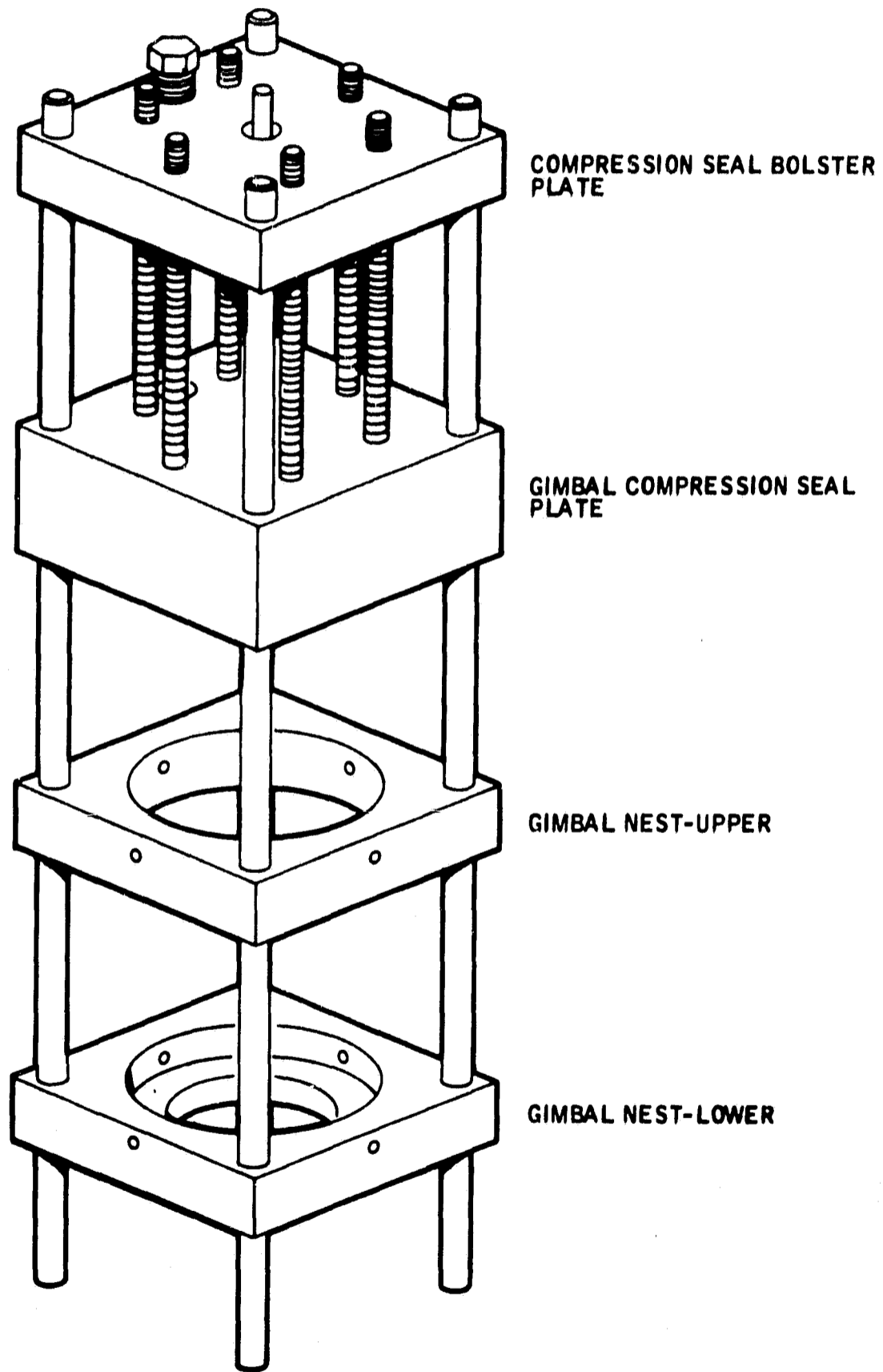


Figure 14. GG159E Gimbal Gas Sampling Fixture

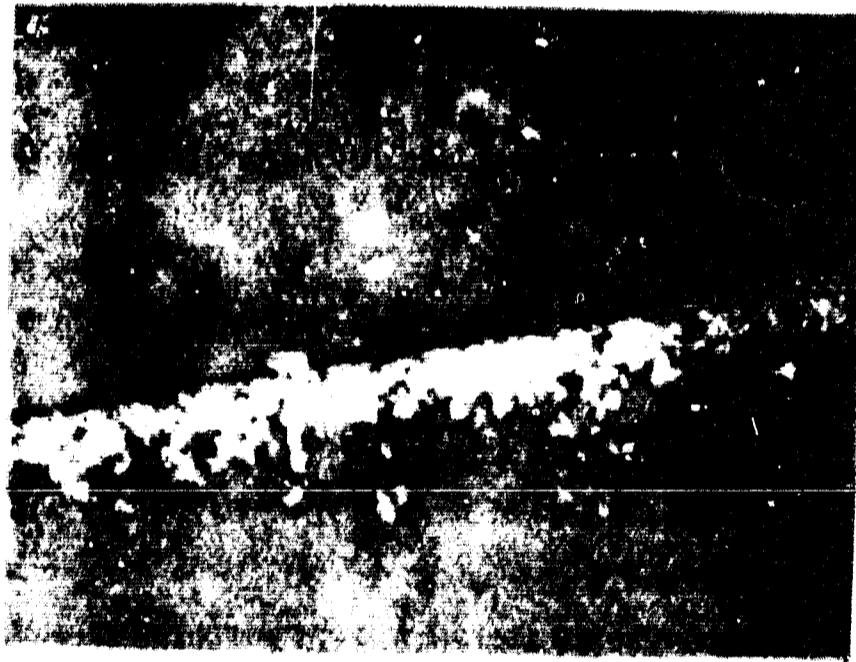


Figure 15. GG159E Contamination

The infrared analysis shown in Figure 16 identified the material composing this ring as MS6293N, a filled epoxy used to impregnate the stator, and MS7381A Bond master which is used to bond the stator laminations. Small particles of these materials evidently came loose from the stator and were drawn to the motor and were deposited there by gas flow.

A new stator was incorporated into the final unit, utilizing metal cans which completely enclose the exposed epoxy. The encased stator is shown in Figure 17. This served to prevent the loose epoxy particles discussed above and to prevent a reoccurrence of variability in starting voltage.

NEW HEADER DESIGN

As a result of the changes in damping fluid and of resulting increased gimbal volume to compensate for the lower density discussed in Section III, the fluid volume increased. Test results on the preliminary gyro build showed that additional bellows travel was necessary to withstand the temperature ranges demanded of this gyro. The test results are shown in Figure 18. The bellows was redesigned with additional displacement capability and was incorporated in the final gyro assembly.

STERILIZATION TEST RESULTS

Test results obtained on the final gyro verified its ability to withstand repeated exposures to sterilization temperature soaks. The data obtained from the test program which included six 64-hour, +135°C (275°F) sterilization cycles is presented in tabular or graphical form as follows:

- Table XI. General Test Parameters

Table XI presents those items which were measured before sterilization testing and remeasured after the six cycles had been completed. No significant performance change will be noted in these test results. Of particular interest is the torquer scale factor, which measured a change of less than 0.02 percent over the six cycles.

- Table XII. Sterilization Test Parameters

Table XII presents those items which were measured before and after each sterilization cycle. This data again shows no excessive shift in any of the parameters, although a nontypical value of fixed torque occurs after the first cycle. For a gyro to shift during the first temperature cycle after build is considered normal, and, as the data shows, such shifts do not continue. Similar, larger than typical first-cycle shifts were seen during the GG 159D1 program and are reported in the final report on that program, 250604-FR1.

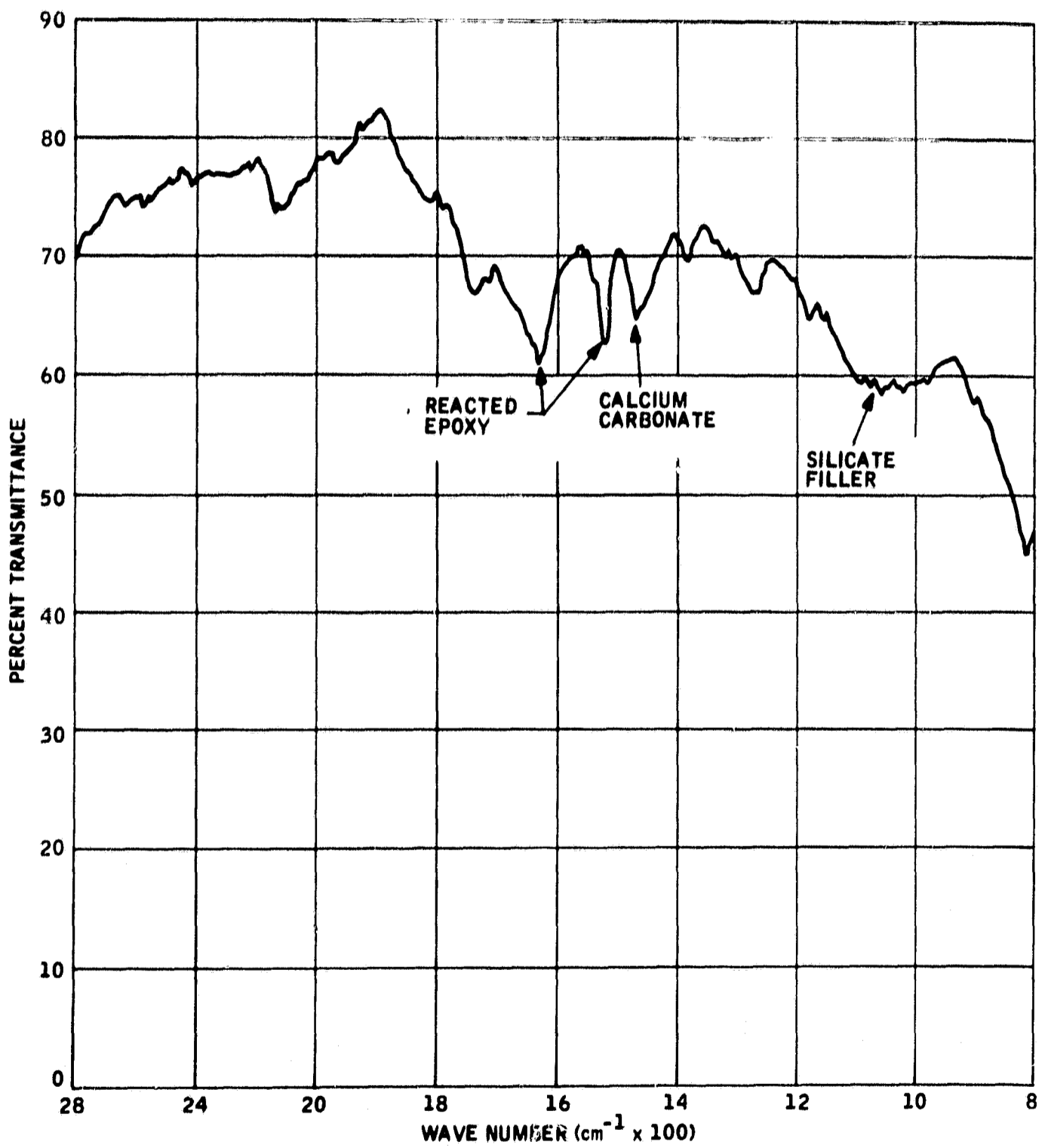


Figure 16. Infrared Spectrum of GG159E Contamination

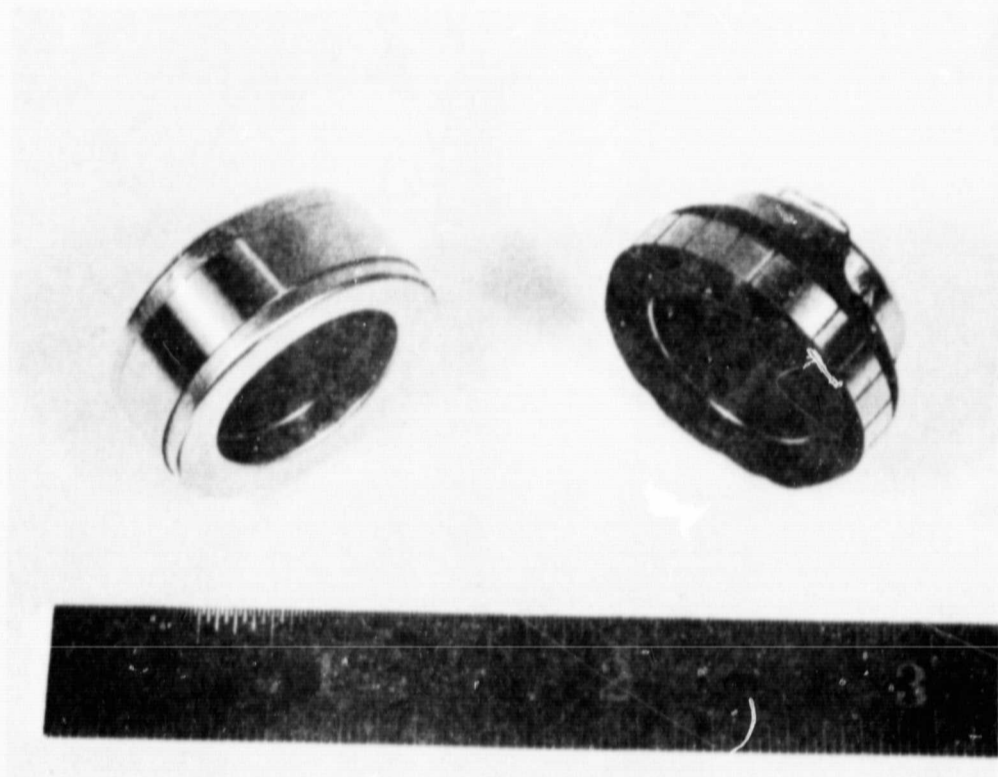
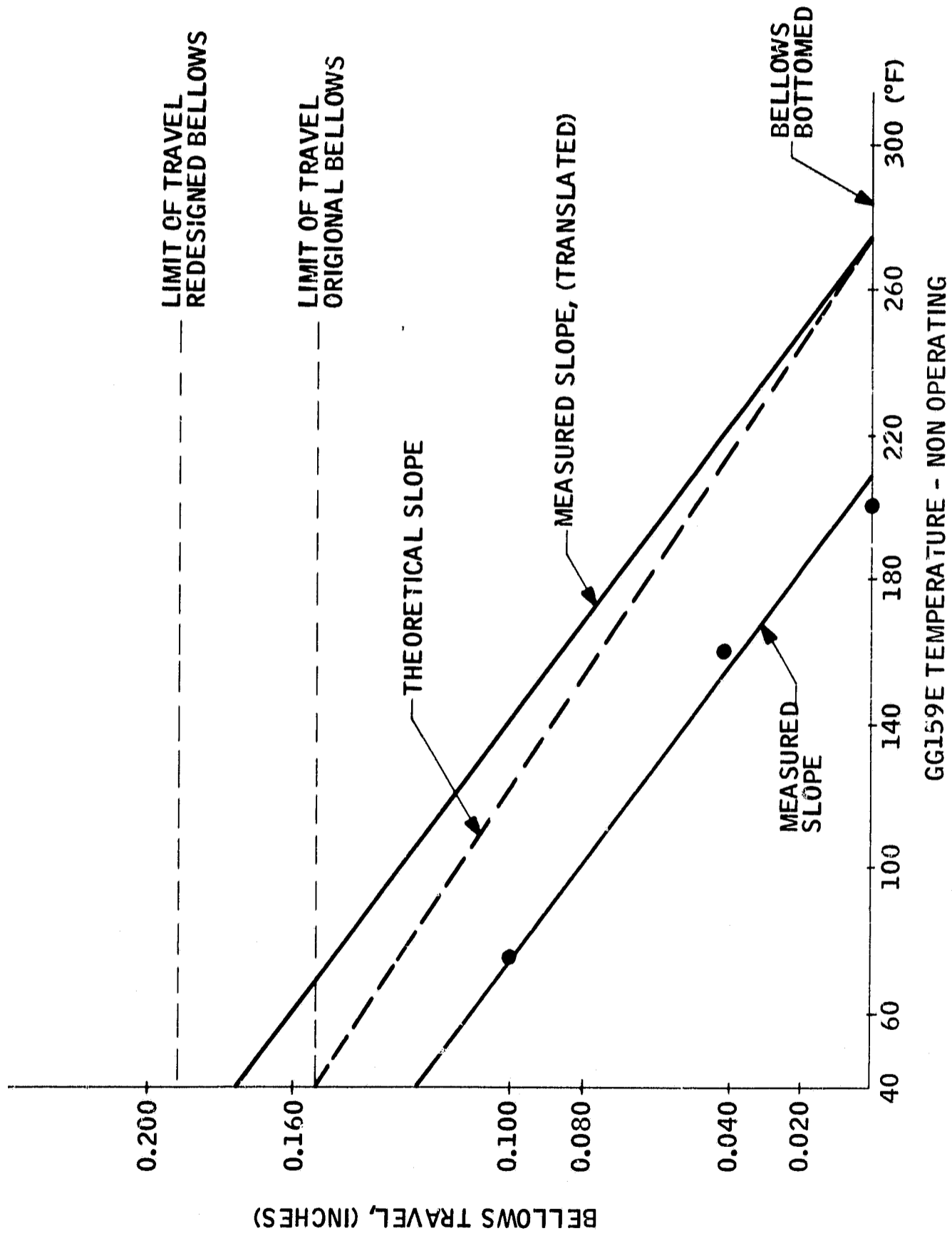


Figure 17. Encased and Standard Motor Stator



GG159E TEMPERATURE - NON OPERATING

Figure 18. Bellows Travel versus Gyro Temperature

- Figure 19. Balance Torque History

Figure 19 presents in a chronological sequence the values of fixed torque, MUSRA, and MUIA measured on the final build of the gyro, including the sterilization cycling. This presentation clearly shows that, except for the normal first-cycle shifts, the gyro performance is not significantly affected by sterilization cycling.

- Figure 20. Step Response

Figure 20 presents the results of the step response testing before and after sterilization. As expected, the nonlinearity due to pivot and jewel clearance is not in evidence, and the response time of approximately 30 msec is invariant over sterilization.

Two difficulties with the hardware, but which are not directly related to performance, did occur during sterilization. These were (1) an open SMRD winding, and (2) degraded balance pan sensitivity.

The open in the SMRD winding was known to be internal to the case. Further investigation would have required a major teardown of the device, and, since the SMRD was not integral to the performance of the unit and the current characteristic of the GBSM lends itself very well to alternate methods of synchronism detection, the matter was judged not to warrant further action at this time. This problem will be better assessed after the sterilization testing which will be accomplished during the GG334S program (JPL Contract 951529) has been completed and the effect on the identical SMRD winding in these gyros has been determined.

The decreased balance pan sensitivity also did not warrant corrective action for this particular unit. The pan had fulfilled its most necessary function at the time of initial trim, and, while retrim at the end of testing is desirable, retrim was not necessary on this unit. Further work to improve the sterilization effect on the balance pan would be in order for future programs.

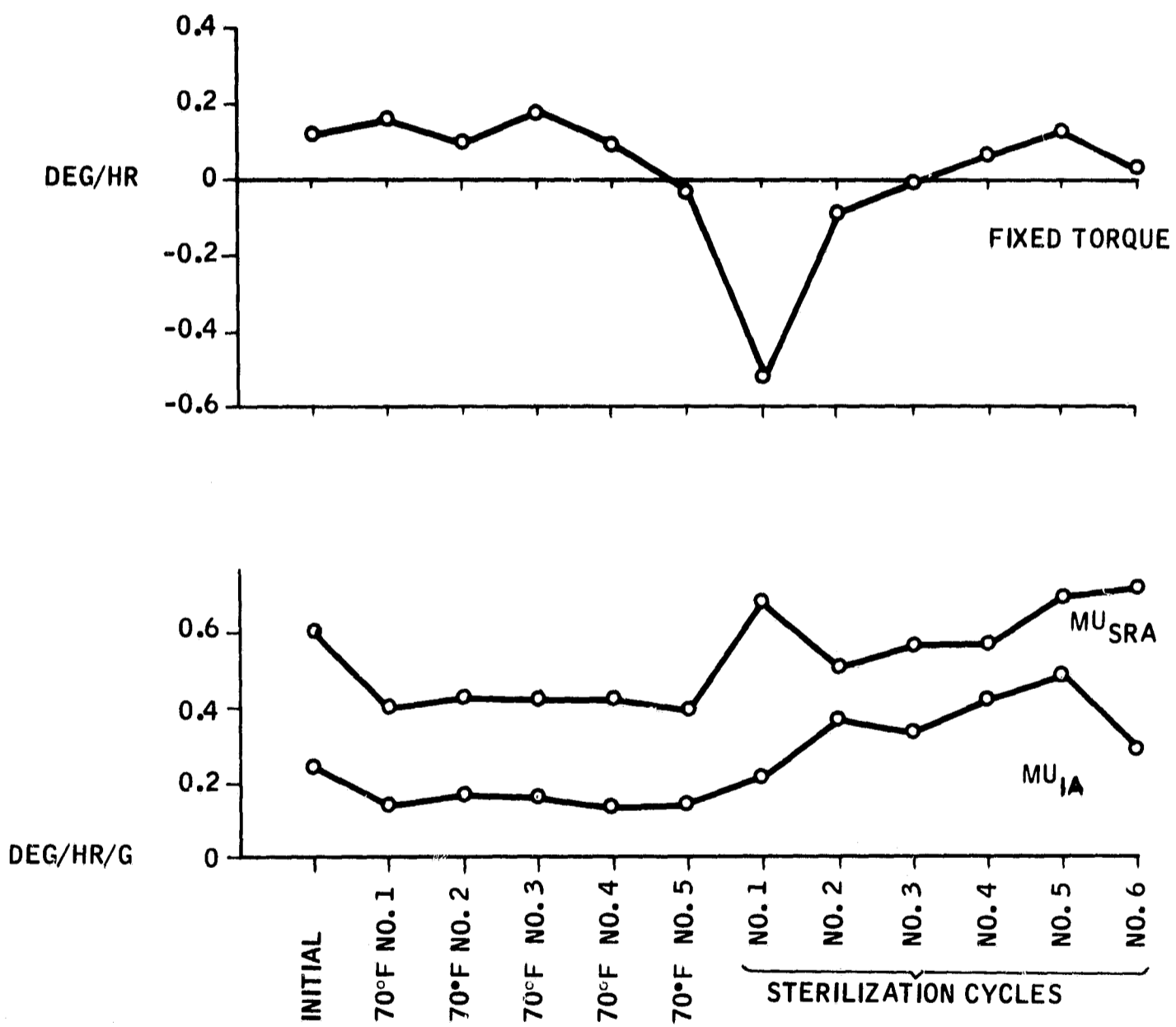
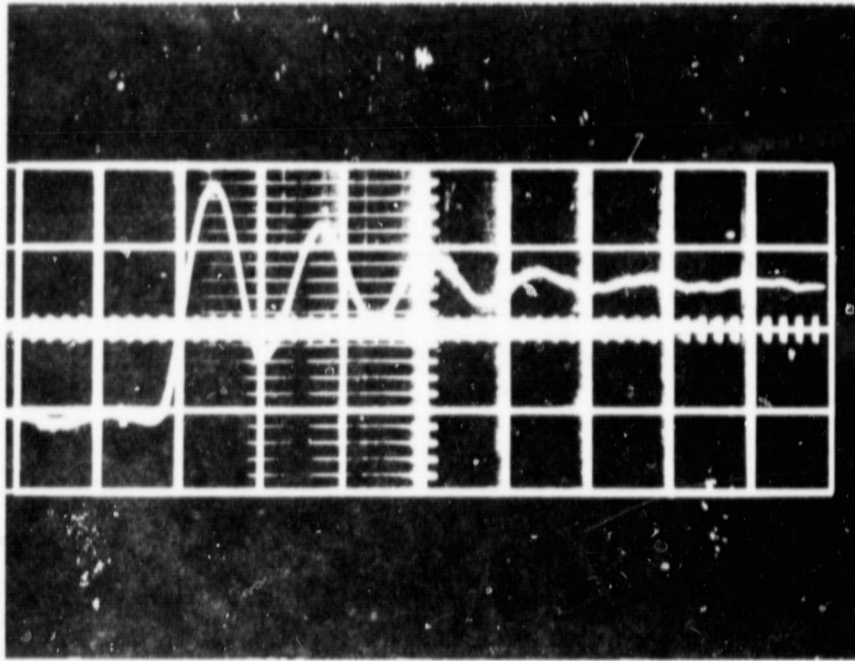
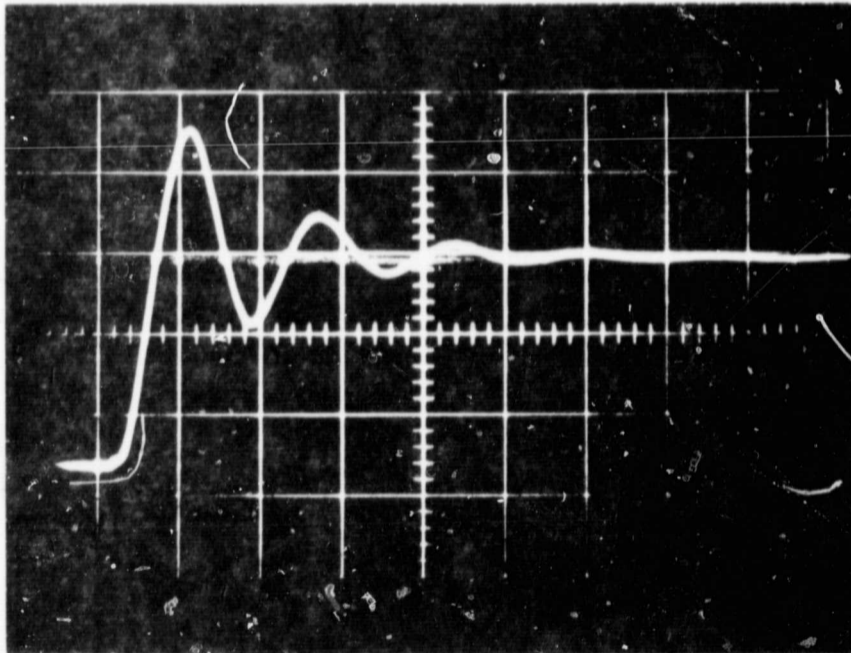


Figure 19. Balance Torque History



Presterilization

Vertical Sensitivity: 2 v/cm
Horizontal Sensitivity: 100 msec/cm



Post-Sterilization

Vertical Sensitivity: 5 v/cm
Horizontal Sensitivity: 100msec/cm

Figure 20. Step Response

Table XII. General Test Results

Parameter	Test Results	
	Before Sterilization	After Sterilization
General Parameters		
Damping (@+115°F)	644 dyne-cm-sec	661.9
Gimbal Freedom	+0.55 -0.56	+0.56 -0.57
Operating Temperature	114.5°F	114.5°F
Spinmotor Power	START 6.8 watts RUN 3.5 watts	6.4 watts 3.4 watts
RUN UP TIME	15.7 sec	15.2 sec
RUN DOWN TIME	56.7 sec	50.3 sec
Spinmotor Torque Margin	5 volts	5 volts
Pickoff Sensitivity	24.12 mv/mr	24.26 mv/mr
Pickoff Null Voltage	1.2 mv	1.3 mv
Torquer		
Scale Factor	356.085 deg/hr/ma	356.15 deg/hr/ma
TSF Stability		0.065 deg/hr/ma
Slew Rate Capability	>11,168 deg/hr	>11,629 deg/hr
Temperature Sensitivity	0.57%	No Requirement
Hydrostatic Pump Frequency	490 Hz	490 Hz
SMRD Output Signal	6.1 mv rms @400 Hz	Open
Drift Parameters	Before Sterilization	After Sterilization
MU	+0.484	+0.709
SRA		
MU	+0.130	+0.287
IA		
RT	-0.030	+0.030
RMS Drift Stability (Run up to Run up)		
OAV	0.050 deg/hr rms	0.041 deg/hr rms
IAV	0.092 deg/hr rms	0.070 deg/hr rms

Table XII. General Test Results

Drift Parameters		Before Sterilization	After Sterilization
Random Drift	OAV (1σ)	0.005 deg/hr	0.003 deg/hr
	IAV (1σ)	0.008 deg/hr	0.003 deg/hr
Elastic Restraint		-0.042 deg/hr/mr	-0.043 deg/hr/mr
Impedances (@115°F)		Before Sterilization	After Sterilization
Spinmotor	ϕ A-C	36.95 ohms	37.10 ohms
	ϕ B-C	35.88 ohms	36.10 ohms
Signal Generator	Primary	30.59 ohms	31.01 ohms
	Secondary	140.7 ohms	141.5 ohms
Torquer	.	161.8 ohms	162.2 ohms
Sensor		780.7 ohms	780.7 ohms
Heaters	Warm Up	278.5 ohms	279.0 ohms
	Control	146.4 ohms	146.7 ohms
SMRD		751.0 ohms	Open
Balance Pan		52.61 ohms	52.25 ohms
Torquer (@ 70°F)		149.2 ohms	149.1 ohms
INDUCTANCES (@115°F)			
Signal Generator	Primary	2.0 mh	1.85 mh
	Secondary	2.0 mh	3.41 mh
Torquer		3.44 mh	3.44 mh
	(@ 70°F)	3.40 mh	3.45 mh

Table XIII. Sterilization Test Results

Parameter	Reference	Post No. 1	Post No. 2	Post No. 3	Post No. 4	Post No. 5	Post No. 6
Random Drift							
OAV (1σ) (deg/hr)	0.005	0.003	0.007	0.001	0.003	0.005	0.003
LAV (1σ) (deg/hr)	0.008	0.002	0.005	0.002	0.004	0.004	0.003
Fixed Torque (deg/hr)	-0.0299	-0.552	-0.092	-0.007	+0.064	+0.125	+0.030
MUI (deg/hr/g)	+0.130	+0.208	+0.370	+0.333	+0.423	+0.485	+0.287
MUS (deg/hr/mr)	+0.484	+0.686	+0.504	+0.563	+0.570	+0.687	+0.709
Elastic Restraint (deg/hr/mr)	-0.042	-0.046	-0.046	-0.048	-0.046	-0.047	-0.043
Run Up time (sec)	15.7	15.0	15.1	15.1	15.0	15.3	15.2
Run Down Time (sec)	56.7	53.6	53.4	51.4	52.4	51.8	50.2
Power							
Start (watts)	6.82	6.50	6.80	6.60	6.70	6.40	6.40
Run (watts)	3.50	3.20	3.35	3.40	3.42	3.35	3.40
Stops (deg OA)	-0.562	-0.561	-0.558	-0.562	-0.562	-0.562	-0.570
	+0.552	+0.552	+0.546	+0.546	+0.551	+0.551	+0.556

SECTION V CONCLUSIONS

Conclusions from the results of the program can be stated as follows:

- 1) The resultant gyro successfully integrated the four major design goals
 - Sterilization capability
 - High-g capability
 - Low-power spinmotor
 - High-frequency pump
- 2) The resultant gyro was a high-grade inertial sensor capable of application to space navigation missions
- 3) Adjustments which are indicated to improve future units are limited in scope and have no substantial impact on the unit performance. These are:
 - a) Elimination or improvement of the SMRD winding
 - b) Improved balance pan
 - c) Adjustment of pump frequency to 400 Hz